

NANOscientific

VOL 19 SPRING 2020

The Magazine for NanoScience and Technology

**HOW COVID-19
DIAGNOSTIC TESTS WORK** p. 6

**NANO INFRARED (IR)
PHOTO-INDUCED FORCE
MICROSCOPY (PIFM)** p. 12

**ELECTROCHEMICAL
AFM (EC-AFM): IN SITU
MONITOR OF COPPER
DEPOSITION/DISSOLUTION
ON GOLD** p. 9

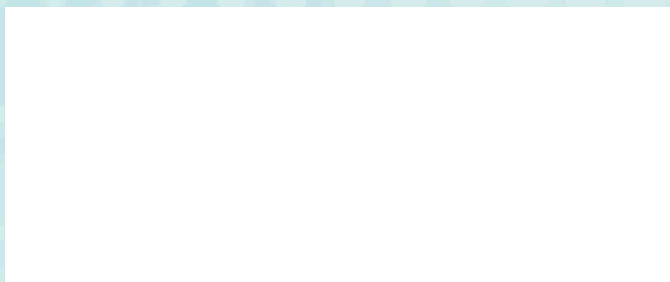


**INDUSTRY NEWS: PARK
SYSTEMS COMPLETES
EQUITY INVESTMENT IN
MOLECULAR VISTA** p. 15

**DETECTION OF
MAGNETIZATION
REVERSAL IN MAGNETIC
PATTERNED ARRAY
USING MAGNETIC FORCE
MICROSCOPY** p. 16

**USING ATOMIC FORCE
MICROSCOPY
IN MEDICAL RESEARCH** p. 21

**PHASE IMAGING OF POLYMER
DEPOSITED ON GOLD** p. 24





The Most Accurate Atomic Force Microscope

Park **NX10** the quickest path to innovative research

Better accuracy means better data

Park NX10 produces data you can trust, replicate, and publish at the highest nano resolution. It features the world's only true non-contact AFM that prolongs tip life while preserving your sample, and flexure based independent XY and Z scanner for unparalleled accuracy and resolution.

Better accuracy means better productivity

From sample setting to full scan imaging, measurement, and analysis, Park NX10 saves you time every step of the way. The user friendly interface, easy laser alignment, automatic tip approach, and analysis software allow you to get publishable results faster.

Better accuracy means better research

With more time and better data, you can focus on doing more innovative research. And the Park NX10's wide range of measurement modes and customizable design means it can be easily tailored to the most unique projects.

To learn more about Park NX10 or to schedule a demo please visit www.parksystems.com/nx10 or email inquiry@parksystems.com



Park
SYSTEMS

TABLE OF CONTENTS

NanoScientific Vol 19

How Covid-19 Diagnostic Tests Work

Euan McLeod, Assistant Professor College of Optical Sciences, University of Arizona

6

Electrochemical AFM (EC-AFM): In Situ Monitor of Copper Deposition/Dissolution on Gold

Jiali Zhang, Ben Schoenek, Byong Kim and Keibock Lee, Park Systems Inc., Santa Clara, CA, USA

9

Nano Infrared (IR) Photo-induced Force Microscopy (PiFM):

a Technique for Nanoscale Hyperspectral Mapping Dr. Sung Park, CEO & Co-Founder, Molecular Vista, San Jose, CA

12

Industry News: Park Systems Completes Equity Investment in Molecular Vista

Detection of Magnetization Reversal in Magnetic Patterned Array using Magnetic Force Microscopy

John Paul Pineda, Byong Kim, and Keibock Lee, Park Systems Inc., Santa Clara, CA, USA

15

16

Using Atomic Force Microscopy in Medical Research

Ana Maria Zasko PhD, AFM core facility manager, UT Health Science Center at Houston, Internal Medicine/Cardiology

21

Phase Imaging of Polymer Deposited on Gold

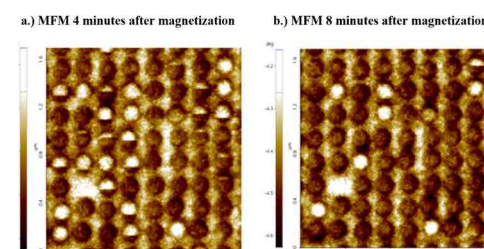
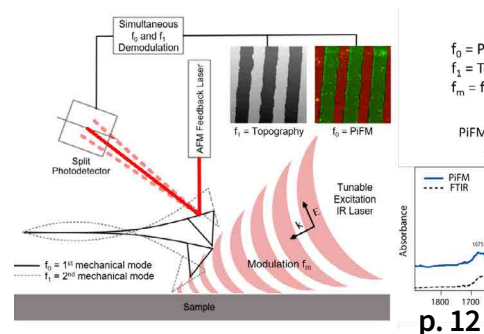
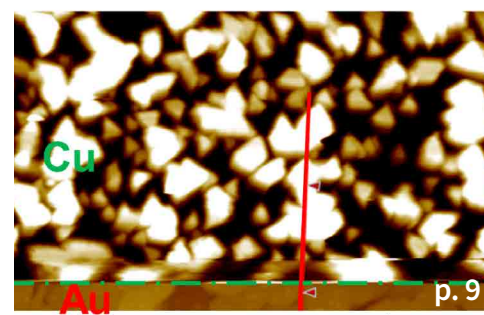
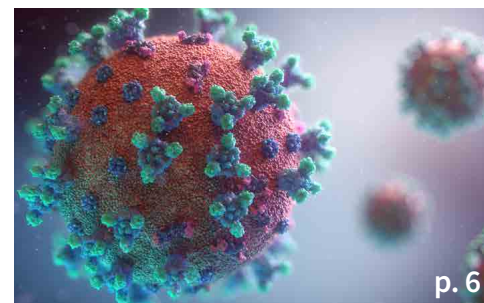
John Paul Pineda, Byong Kim, and Keibock Lee, Park Systems Inc., Santa Clara, CA, USA

24

Materials Matter - Column 4 - Flexible Nano Electronics

Dr. Rigoberto Advincula

27



MESSAGE FROM EDITOR

In this issue, we look into the COVID-19 testing and nano particle interactions through the lens of scientists researching the virus. We have articles examining the interaction between light, molecules and nano particles, and techniques and tools used in research labs detecting electrochemical reactions and nano infrared mapping. Wide-ranging applications of AFM in medical research show us the relevance of nano tools at the fingertips of scientists that uncover the mysteries once left only to speculation about cell biology.

We hope you enjoy this issue and also want to invite you to submit an abstract

for the NanoScientific Symposium on Nano Materials for a Changing World (see p. 26) where we invite speakers to present their research on various applications from electrochemistry for clean energy, biotechnology on virus and cancer research for saving lives, and other nanomaterial studies for supporting better life and improving the world.

If you are a researcher at a national lab or academic institution, we invite you to apply for a Park Nano Research Grant, which gives access to Atomic Force Microscopes to researchers setting up a lab.

We offer a sincere wish for your safety during this very challenging time and appreciate your support of our publication.

Keibock Lee
Editor-in-Chief

NANOScientific 2020 EDITORIAL BOARD



Dr. Rigoberto Advincula, Professor, Department of Macromolecular Science and Engineering at Case Western Reserve University.



Dr. Lane Baker, James L. Jackson Professor of Chemistry Indiana University



Mr. Phil Kaszuba, Global Foundries Senior Member of Technical Staff and lead engineer in their Scanning Probe Microscopy (SPM) laboratory.



Dr. John A. Marohn, Professor & Director of Undergraduate Studies, Department of Chemistry and Chemical Biology Member, Field of Materials Science & Engineering, Cornell University.



Dr. Ye Tao, Rowland Fellow & Principle Investigator, Rowland Institute of Science at Harvard University, BA Harvard in Biochemistry, PhD MIT/ETH Zurich Chemistry



Dr. Gwo-Ching Wang, Travelstead Institute Chair, Dept. of Physics, Applied Physics & Astronomy, Rensselaer Polytechnic Institute.



Dr. Jiahua Jack Zhu, PhD, University of Akron, Associate Professor, Department of Chemical and Biomolecular Engineering.



Dr. Yiping Zhao, Professor, Department of Physics and Astronomy, Director, Nanoscale Science and Engineering Center, The University of Georgia.

ONLINE NanoAcademy

Live Demos, Webinars and Seminars from AFM experts collected in one place.

Easily join a live session or review on-demand content from home!



Visit parksystems.com/onlineNanoAcademy

NANOscientific

Keibock Lee, Editor-in-Chief
kei@nanoscientific.org
Debbie West, Content Editor
debbiewest@nanoscientific.org
Byong Kim, Technical Director
Debbie Bishop, Art Director
Richard Oettinger, Marketing Manager

Publisher & Corporate Officers
Park Systems Corporation
Sang-il Park, Chief Executive Officer
Karen Cho, VP of Finance
Keibock Lee, President
Park Systems, Inc.
3040 Olcott Street
Santa Clara, CA 95054
inquiry@parksystems.com
www.parksystems.com

NANOscientific is published quarterly to showcase advancements in the field of nanoscience and technology across a wide range of multidisciplinary areas of research. The publication is offered free to anyone who works in the field of nanotechnology, nanoscience, microscopy and other related fields of study and manufacturing.

We would enjoy hearing from you, our readers. Send your research or story ideas to debbiewest@nanoscientific.org

To view all of our articles, please visit our web site at www.nanoscientific.org

INSET PHOTO ON COVER: Phase image overlaid on topography after heating a polymer sample at elevated temperature of 230 °C and applying 1 V DC voltage between the polymer sample and the tip. The topography acquired after the heat and bias treatment reveals that two circular protrusions (inner and outer protrusions) formed in the center of the scanned surface. The inner circular protrusion has a height of around 53 nm and a diameter ranging from 1.4 μm to 2.0 μm. The outside circular protrusion has a lower height of around 30 nm and a diameter ranging from 2.0 μm to 4.0 μm.

The surrounding area is relatively flat with a mean square surface roughness of 0.8 nm. By comparing topography and phase image, it could be observed that the orientation of the lamellar fibrils in the inner and outer circular protrusions is rearranged and the fibrils are aligned differently in both protrusions as well as the flat surface.



HOW COVID-19 DIAGNOSTIC TESTS WORK

Colin J. Potter and Euan McLeod

Colin J. Potter and Euan McLeod

Wyant College of Optical Sciences
University of Arizona
Tucson, AZ 85721

In the last several months, COVID-19 has challenged countries around the world as governments and health systems struggle to contain the spread of the disease and to mitigate its impact. The worldwide response has been remarkable, with nations implementing policies to limit human-to-human spread, distribute and manufacture hospital resources, and ensure that citizens' basic needs are met. Of all the measures implemented to combat the COVID-19 pandemic, possibly the most impactful is the rapid and early detection of the virus that causes it, SARS-CoV-2, which can inform the need for quarantine, treatment, and contact tracing of infected individuals (Kochańczyk, 2020).

Testing at the desired scale is no easy task, as we have seen in the US and other countries around the world. The scarcity of available test kits, their accuracy and sensitivity, the delay in receiving results, and the relative complexity of the tests themselves all stand as barriers to widespread testing. The development

of new, more sensitive, and specific diagnostic technologies has enabled better testing now than was available for the SARS outbreak in the early 2000s, but there is still significant room for improvement.

RT-PCR as a powerful diagnostic tool

Currently, testing for the SARS-CoV-2 virus in the US and around the world is dependent on the use of an approach called reverse transcriptase quantitative polymerase chain reaction (RT-qPCR) or real-time reverse transcriptase PCR to detect the presence of the virus (CDC, 2020). RT-qPCR is performed on a sample taken from a patient, most often a swab of the patient's upper respiratory tract. The sample is processed to isolate any genetic material in the form of nucleic acids, including human DNA from the patient themselves and any positive-sense RNA present, the genetic material of the SARS-CoV-2 virus.

In RT-qPCR, this RNA is converted into complementary DNA, and then amplified and detected by fluorescence from a DNA binding dye or by a fluorescent DNA probe that binds to a specific sequence of target DNA. The amplification process

requires heating and cooling of the sample in a small chamber, with each cycle doubling the amount of target DNA and thus the amount of fluorescence. Practically, RT-qPCR has demonstrated a limit of detection of 1 copy of RNA per μL in a 30 μL sample (CDC Diagnostic Panel, 2020). With high specificity (i.e. no false positives) based on the use of known primer strands for SARS-CoV-2 RNA, RT-qPCR is a powerful tool for diagnosing viral infections. However, as COVID-19 continues to spread, some aspects of RT-qPCR have stood as barriers to its rapid and effective implementation.

Diagnosis of COVID-19 using RT-qPCR typically requires sophisticated laboratory equipment and expertise, resulting in a long delay between testing and obtaining results. During this time, a patient may have already spread the virus to several other people, presenting a major problem in the control of an epidemic. Devices such as ID NOW™ and POKKIT™ are relatively new technologies that utilize insulated isothermal polymerase chain reaction, or iPCR, to qualitatively detect the presence of pathogen RNA (Tsai, 2014). In these devices, the sample is heated from the bottom, creating a

convection current where it cools as it moves up in the chamber, effectively providing the heating and cooling cycles of traditional PCR. While this has enabled rapid, point-of-care diagnostic PCR testing to become a reality, it can only give a qualitative result (the presence or absence of pathogen) and is 10-100 fold less sensitive than conventional RT-qPCR (Zhang, 2016).

Additionally, other indications of infection and immunity such as antibodies that the body produces to defend against the virus cannot be detected by either RT-qPCR or iPCR, so the virus itself must be sampled to detect infection. Besides antibodies, the body also responds to infection by producing cytokine molecules that trigger an inflammatory response. In severe cases, too many cytokines can result in a potentially lethal cytokine storm. In COVID-19, the viral load in upper respiratory secretions has been shown to vary significantly between patients (Zou, 2020), indicating that detecting viral RNA alone may not be as effective at diagnosing COVID-19 as a test that can simultaneously detect antibodies and other biomarkers.

The perfect COVID-19 diagnostic test

An ideal test for COVID-19 would accomplish several things. One, it should be able to rapidly detect the presence of the viral particle. Two, it should give us information about any antibodies and cytokines that the patient has produced against the virus. Three, it should be sensitive enough to detect even small quantities of these targets in asymptomatic or early infections. Four, it should be administered at the point of care, preferably in an easy-to-use handheld or wearable device that gives results on the spot. And finally, it should be inexpensive enough to be mass produced for the deployment of millions of tests. Such a device would limit user error and testing variability and ultimately enable rapid identification and containment of new outbreaks.

Detecting beyond RNA with ELISA

One testing method that is already widely used is an enzyme-linked immunosorbent assay (ELISA). In this method, antibodies tagged with enzymes are used to detect target protein molecules in a sample [Fig 1]. This is quite different from PCR,

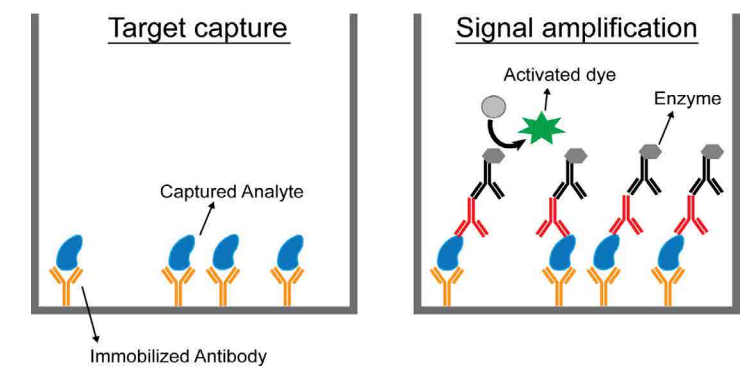


Figure 1: Biosensing using a sandwich ELISA. The target analyte is captured using immobilized antibodies that are reactive against the analyte. All unwanted protein is then washed off before the application of primary and secondary antibodies, which are tagged with enzymes. Signal amplification occurs via enzyme conversion of a dye to a visible form that can be detected and quantified.

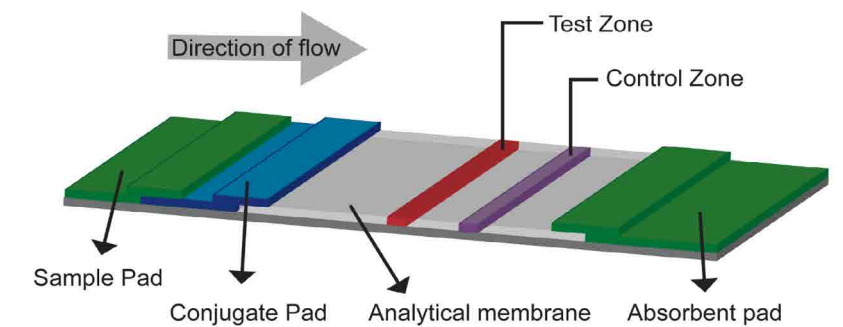


Figure 2: Lateral flow assay (LFA) biosensor. A liquid sample is placed on a sample pad, which then migrates via capillary action to a conjugate release pad, where it can pick up labeled or dye-tagged antibodies that bind specifically to the target analyte to form an antibody-analyte complex. This complex then migrates across a porous membrane towards the detection zone, where a test line containing immobilized anti-analyte antibodies captures the complex, if present. The control zone tests for adequate flow by using another set of antibodies to capture any of the tagged antibodies from the conjugate pad that make it past the test zone.

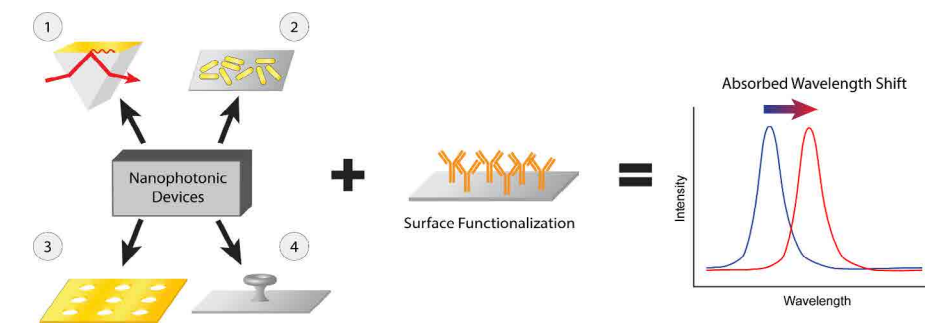


Figure 3: Nanophotonic biosensors. Structures with optical resonances for a particular wavelength of light are fabricated and functionalized with antibodies designed to capture a target molecule. When that target binds to the surface of the sensor, it perturbs the local refractive index, and the resonant wavelength shifts, providing a detectable signal for the sensor. 1- Basic surface plasmon resonance (SPR) detector using gold film on a prism (Liedberg, 1983). 2- Localized SPR, gold nanorod detector (Mayer, 2008). 3- Plasmonic nanohole array (Cetin, 2015). 4- Microtoroid optical resonator (Su, 2016).

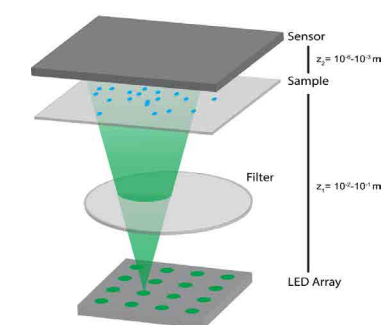


Figure 4: Lens-free holographic microscopy. Light from the LED array illuminates the sample, then is collected after diffracting through objects in the sample field. The sample image is computationally reconstructed to identify particles in the sample plane and generate an image similar to that from a conventional microscope. The ability for this system to be compacted into a handheld device makes it a powerful diagnostic tool.

which can only detect DNA or RNA.. Each enzyme can change the color of many dye molecules, resulting in signal amplification, which makes ELISA quite sensitive. While ELISA is not currently widely used to detect SARS-CoV-2 due to the success of RT-qPCR, it still has the potential to be a powerful diagnostic tool in the fight against this and future pandemics.

ELISA has some of the same barriers as PCR when it comes to effective implementation, particularly during an epidemic. ELISA also requires quantitative detection using laboratory machinery with trained staff, and it is more complex than RT-qPCR, requiring controlled storage conditions for the antibodies and leading to similar delays as RT-qPCR from initial testing to results.

Simple point-of-care technologies

Lateral flow assays (LFAs), based on a similar technology as over-the-counter pregnancy tests, can also be used to detect the SARS-CoV-2 virus [Fig 2]. If present, an analyte-antibody complex presents itself as a colored line that indicates a positive test.

The main draw of such a diagnostic technology is that it can be administered and read at the point of care to detect both proteins and RNA/DNA (through use of complementary DNA strands instead of antibodies). Widespread implementation of LFAs could help to control the spread of COVID-19 by providing an instant result. Unfortunately, the main drawback of LFAs is their sensitivity. Due to the design of LFA tests, there is currently no way to amplify a signal, leading to a sensitivity that cannot compete with that of PCR and that is limited by the amount of sample used (Bishop, 2019). Additionally, LFA tests that use new reagents to detect new biomolecules are difficult to produce and optimize, further limiting the usefulness of such technology in the face of a novel pathogen like SARS-CoV-2.

Sensing the future

As we continue to push for sensitive, compact, point-of-care diagnostic technologies, the field of nanophotonic biosensors has made great strides in accomplishing these goals. The potential of these sensors makes them attractive as future diagnostic tools. Nanophotonic biosensors utilize unique material structures to confine light to small volumes in order to increase the interaction between

the light and the target analyte. Often, nanophotonic biosensors rely on the same DNA or antibody capture molecules used in the previous techniques; however, the detection of the captured molecule is performed optically, which can enable extreme sensitivity in a field-portable package. Devices based on a variety of different material structures have been used that provide limits of detection in the nanomolar to attomolar concentration ranges, including solid metal films (surface plasmon resonance), perforated metal films, arrays of metallic nanoparticles, or glass microstructures where the light skirts their circumference in a whispering gallery mode [Fig 3]. In principle, such technology can be made small and portable, capable of containing all the components necessary for analyte detection in a small chip. These emerging point-of-care technologies are at the forefront of diagnostic biosensing and, with the proper configuration, could be used to detect SARS-CoV-2 surface proteins, RNA, or even antibodies against the virus.

An alternative technology that we are developing employs an emerging form of microscopy called lens-free holographic microscopy [Fig 4]. This technology has the potential to detect a wide dynamic range of analyte concentration, prioritizing both sensitivity and versatility of detectable particles (Xiong, 2018). By using a lens-free system, imaging of this kind can be compacted into a cost-effective hand-held device capable of imaging a sample at sub-micron resolution over a field of view of 20 mm x 20 mm. Reconstruction of the microscopic image is accomplished by computationally processing a recorded diffraction pattern. This enables the detection of nanoscale particles, which can be configured to bind to target biomolecules. This chip-scale sensing approach can form an economically-viable point-of-care diagnostic tool with a high sensitivity to detect the SARS-CoV-2 virus itself as well as the body's response to the infection.

While there is still some work to be done before these technologies can be implemented on a large scale, we currently stand on the edge of a new era of diagnostic medicine. As new innovations in biomedicine become available, we will be able to detect disease, mitigate the impact of future pandemics, and target personalized medicine using these sensitive and versatile biodetection systems.

Author Biographies:



Colin Potter is an M.D./Ph.D. student studying Optical Sciences in the Wyant College of Optical Sciences at the University of Arizona (UA). He received his B.S. in Neuroscience from UA in 2018 where

he studied the effects of parasitic invasion into the brain on the central nervous system. He began studying medicine at the UA College of Medicine Tucson in 2018 and joined the lab of Dr. Euan McLeod to study soft nanophotonic systems and their applications in biodetection.



Euan McLeod is an Assistant Professor in the Wyant College of Optical Sciences at the University of Arizona (UA) since 2015. He is also an Assistant Professor of the UA BIO5 Institute and an Affiliate Member

of the UA Cancer Center. He has received postdoctoral training at UCLA and Caltech. He received his Ph.D. from Princeton University and his B.S. from Caltech. Euan's background and interests lie at the intersection of optics, nanoscience, and soft bio-materials science.

References:

- Kochańczyk M, Grabowski F, and Lipniacki T, "Impact of the contact and exclusion rates on the spread of COVID-19 pandemic," medRxiv (2020). Centers for Disease Control and Prevention, "CDC Tests for COVID-19," (2020). Centers for Disease Control and Prevention, "CDC 2019-Novel Coronavirus (2019-nCoV) Real-Time RT-PCR Diagnostic Panel," Catalog # 2019-nCoV-EUA-01 (2020) Tsai YL et al., "Validation of a Commercial Insulated Isothermal PCR-based POCIT Test for Rapid and Easy Detection of White Spot Syndrome Virus Infection in Litopenaeus vannamei," PLOS One 9, e90545 (2014). Zhang J et al., "Evaluation of two singleplex reverse transcription-insulated isothermal PCR tests and a duplex real-time RT-PCR test for the detection of porcine epidemic diarrhea virus and porcine deltacoronavirus," J Virological Methods 234, 34-42 (2016). Zou L et al., "SARS-CoV-2 Viral Load in Upper Respiratory Specimens of Infected Patients," New England Journal of Medicine 382, 1177-1179 (2020). Bishop JD, Hsieh HV, Gasperino DJ, and Weigl BH, "Sensitivity enhancement in lateral flow assays: a systems perspective," Lab on a Chip 19, 2486-2499 (2019). Soler M, Calvo-Lozano O, Estevez MC, and Lechuga LM, "Nanophotonic Biosensors Driving Personalized Medicine," Optics and Photonics News, 26-31 (2020). Leidberg B, Nylander C, and Lundstrom I, "Surface Plasmon Resonance for Gas Detection and Biosensing," Sensors and Actuators 4, 299-304 (1983). Mayer KM et al., "A Label-Free Immunoassay Based Upon Localized Surface Plasmon Resonance of Gold Nanorods," ACS Nano 2, 687-692 (2008). Cetin AE et al., "Plasmonic Nanohole Arrays on a Robust Hybrid Substrate for Highly Sensitive Label-Free Biosensing," ACS Photonics 2, 1167-1174 (2015).

APPLICATION NOTE

ELECTROCHEMICAL AFM (EC-AFM): IN SITU MONITOR OF COPPER DEPOSITION/DISSOLUTION ON GOLD

Park SYSTEMS

Jiali Zhang, Ben Schoenek, Byong Kim and Keibock Lee, Park Systems Inc., Santa Clara, CA USA

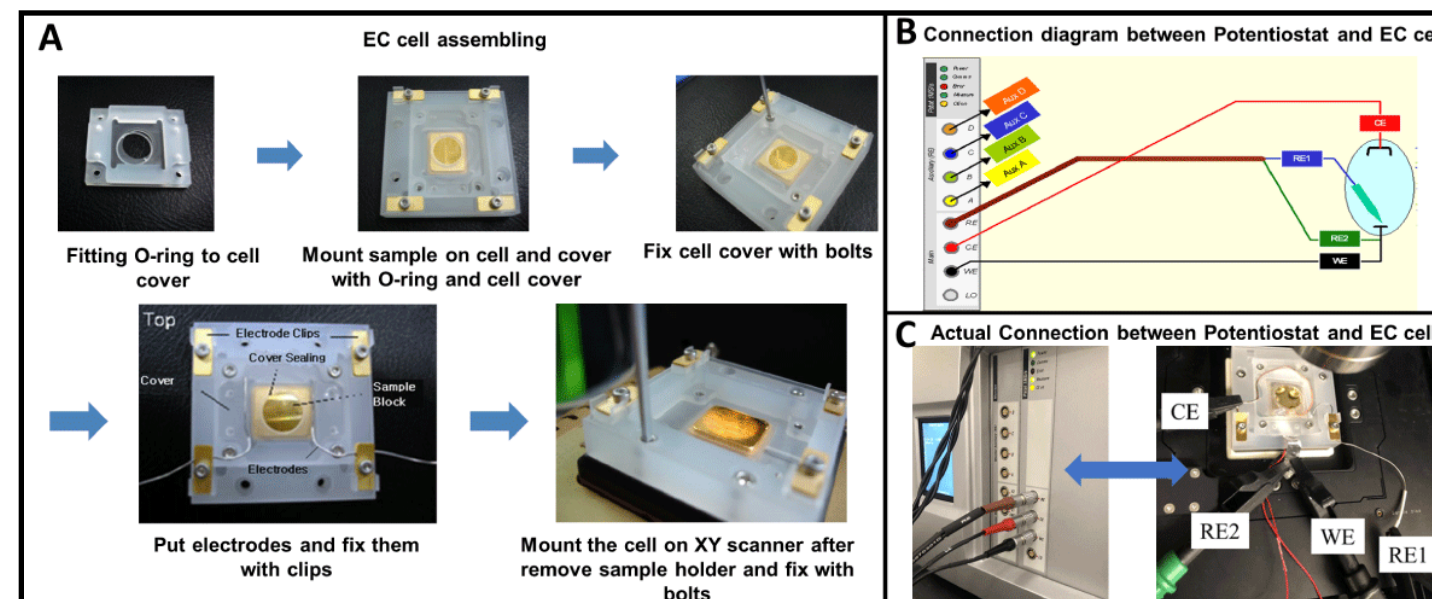


Figure 1. Experimental setup: (A) A step-by-step guide to assemble an EC cell before mounting to the Park AFM system; (B) Schematic diagram showing how to connect the potentiostat with the assembled EC cell; (C) Close-up of Au (111) working electrode mounted inside an EC cell and fixed on a Park NX12 stage while connected to the potentiostat following the above diagram.

Introduction

Electrodeposition is emerging as a popular way to fabricate electronic nanostructures on a surface [1, 2]. Understanding and controlling this process at nanoscale has been a long-standing challenge in electrochemistry. Atomic force microscopy (AFM) has proven to be a versatile tool to characterize and manipulate surface features with nanometer resolution. Researchers are therefore motivated to combine electrochemical experiments and AFM technology into electrochemical AFM (EC-AFM). This combination allows the researcher to perform in situ analysis, and control the electrochemical reactions at solid-liquid interfaces [3-5]. This technique has been used in applications as varied as battery studies [5-7], metal corrosion [8, 9], biosensor development [10], and more.

This study shows the investigation of localized electrochemical deposition and dissolution of copper using EC-AFM. In the study, a Park NX12 AFM system is equipped with a three-electrode electrochemical cell (EC cell) connected to a potentiostat. A conductive Au (111) surface is used

as a working electrode (WE) where the electrochemical reaction takes place. The deposition process, at low potential, and dissolution, at high potential, are shown to be fully reversible, rapidly – within one AFM scan line. This simultaneous topographic image and electrochemical response was recorded. Our results demonstrate that EC-AFM can be used for monitoring the in situ electrodeposition process and also obtain insight into controlled additive nano-fabrication of an EC reaction at the solid-liquid interface.

Experimental

A Park NX12 was used to monitor the deposition and dissolution of copper on an Au surface. The measurement principles and major parts of the EC-AFM setup are similar to using AFM in liquid. A non-conductive probe (CONTSC cantilever with spring constant of 0.2 N/m) was employed and mounted on a Teflon chip carrier, which was mounted onto a liquid proband designed by Park Systems. This setting ensures that it does not interfere with the electrochemical reaction. All of the AFM topographic images shown were

characterized using contact mode in electrolyte solution, using a force of 5 nN and a scan rate of 0.5 Hz.

Au (111) on mica was mounted in an EC cell made of Polychlorotrifluoroethylene (PCTFE), manufactured by Park Systems. The substrate was mounted with a top cover and securely sealed with a thin, silicon O-ring to prevent leaking, following the step-by-step procedure shown in Figure 1A. After the EC cell was well assembled, the electrode cables were connected between the potentiostat (Solartron Modulab XM, Ametek Solartron, UK) and the EC cell based on the connection diagram (Figure 1B). Three cables were connected: WE, reference electrode (RE) and counter electrode (CE). In this study, a silver chloride electrode (Ag/AgCl) is used as the RE which keeps the potential between itself and the working electrode constant. Typically, Platinum-Iridium (Pt-Ir) wires can be used as the CE. Here Cu wire acted as the CE due to its excellent malleability. When the WE area is bigger than the CE area, a signal saturation error occurs in the potentiostat. Typically, the CE was reshaped into a ring

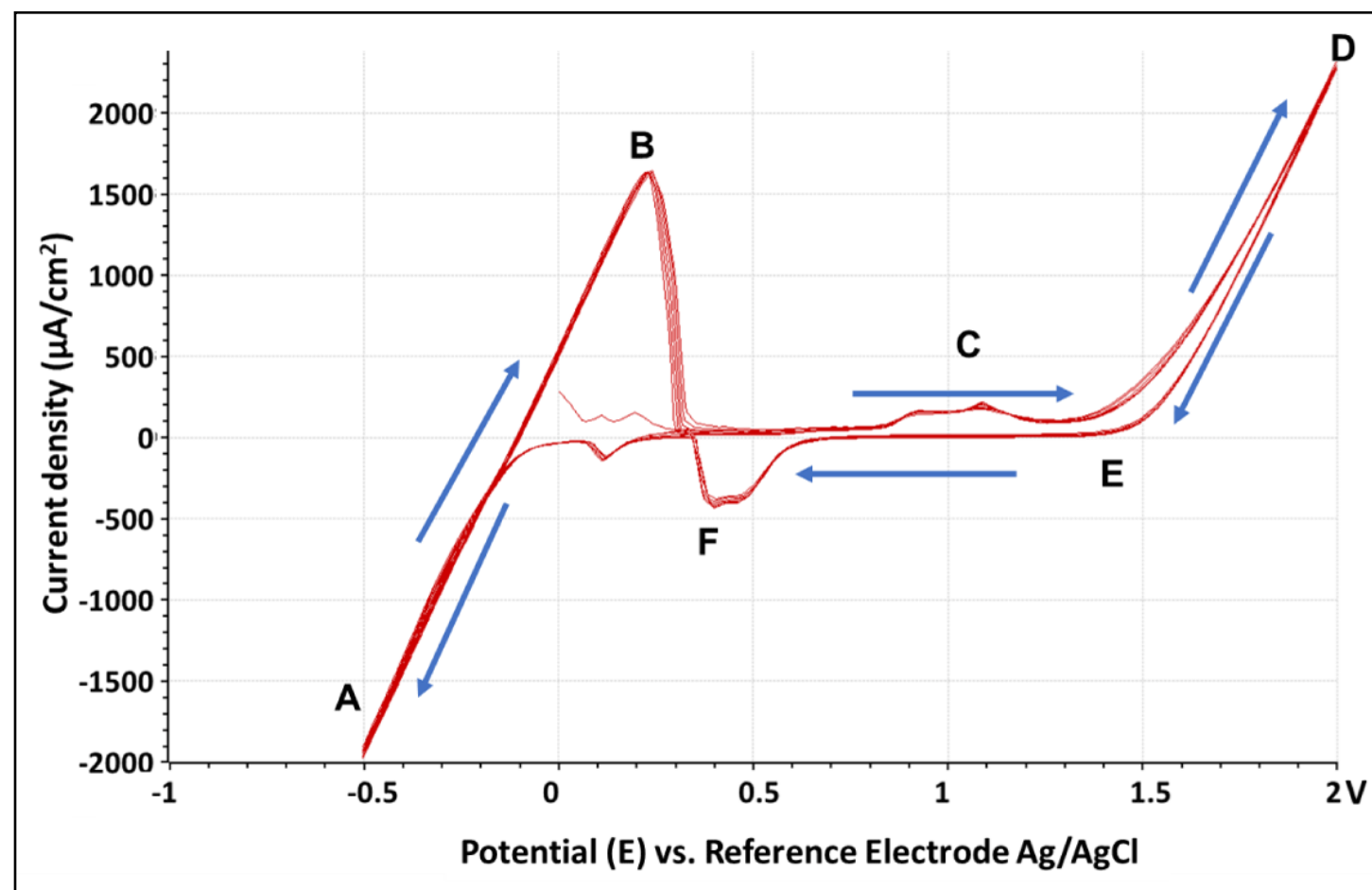


Figure 2. Cyclic voltammograms: The CV curve was taken with an Au electrode mounted in a Park AFM EC cell measured in 20 mM CuSO_4 solution.

to increase the CE area, as shown in Figure 1C. All of the electrodes were isolated from each other. After the experimental setup was ready, an electrolyte solution (20 mM CuSO_4) immersed the electrodes inside the EC cell.

After the cell was assembled, the cyclic voltammetry (CV) technique was employed to investigate the electrochemical reaction mechanisms. These mechanisms give rise to electroanalytical current signals by applying a voltage to the CE immersed in electrolyte solution. The cyclic voltammograms generated from the software are displayed as the curve for the current vs. the potential for a linear potential sweep. The sweep of CV was set to -0.5 V to 2 V, with a sweep rate of 100 mV/s for ten cycles. Current density was calculated using the geometric area of the electrode by the Modulab ECS software. CV measurement was used to understand and control the redox reaction.

Results and Discussion

A reversible CV curve was generated after successful setup. Based on the cyclic

voltammogram generated (Figure 2), as the potential was scanned positively from point A to point D, the oxidation reaction (dissolution of copper) occurred. When the switching potential (D) was reached, the scan direction was reversed (from D to F), and the potential was scanned in the negative direction where the reduction reaction occurred. This happened when the copper was deposited on the Au surface. The sweep was steadily run for 10 cycles as shown by the overlapping of the 10 traces. As a result, one can find the threshold potential of copper deposition (-0.5 V) and dissolution (2 V) based on the CV curve.

The EC-AFM allows the recording of the topographic changes during electrodeposition/dissolution of materials on the surface. The AFM images in Figure 3 are the topographic images recorded before deposition (Fig. 3A), during deposition (Fig. 3B) and after dissolution of copper (Fig. 3C). As shown in Figure 3A, the bare gold surface with visible terraces was first imaged via AFM. Then the lower limit voltage was constantly applied to the electrode ($E = -0.6$ V), when a great morphology change

showing copper deposition was clearly observed in Figure 3B. The deposition rate increased with time. As the image was scanned from top to bottom, with the time increasing, the deposited copper clusters grew bigger and bigger in size as well. This deposition of copper was reversible. When a higher voltage of 3V was applied for five minutes, the bare Au underneath was again exposed (Figure 3C). All three images were scanned at the same area to confirm the occurrence of copper deposition and dissolution. The Au domains remained the same, as shown by comparing A and C, thus confirming that this electrochemical process is fully reversible.

The in situ dissolution of copper was also monitored with AFM. In the middle of the imaging, positive voltage was applied at the position of the horizontal green dashed line. Tall copper islands (up to 75 nm) dissolved, exposing the bare Au surface (Figure 4). This morphologic change in the middle of the image was clearly characterized via AFM. Likewise, one can also record the in situ deposition using AFM by shifting it to negative voltage.

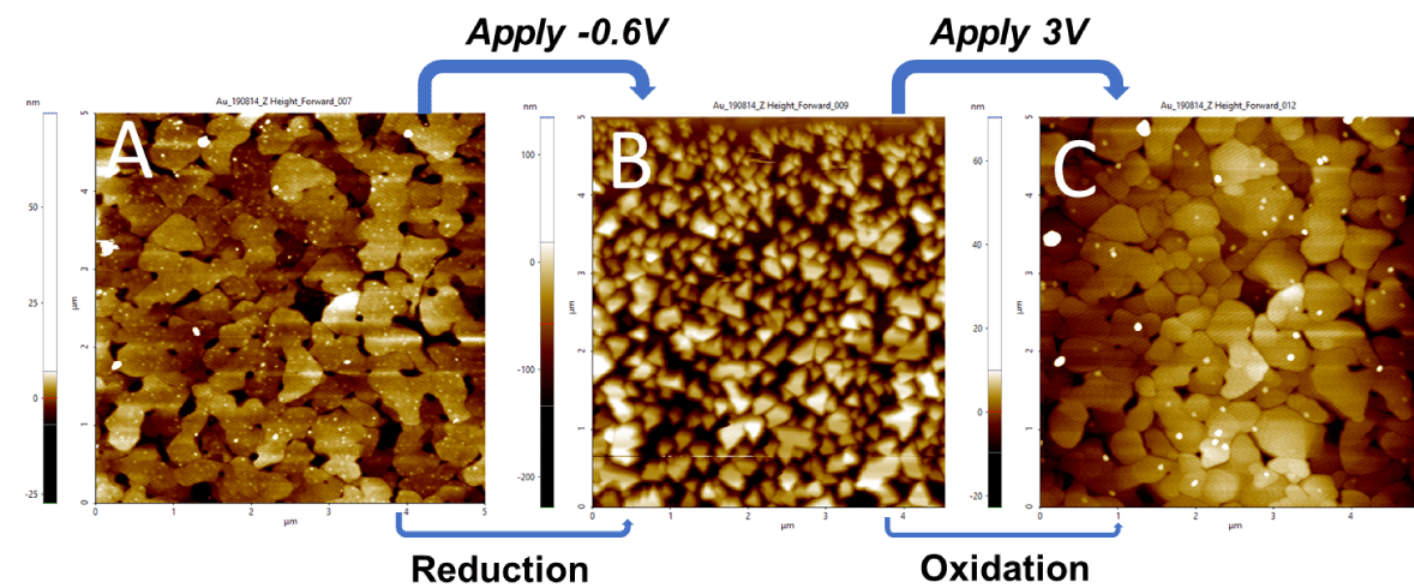


Figure 3. (A) Pristine Au surface before applying voltage; (B) After applying -0.6V through the potentiostat, the Au surface was covered with copper clusters; (C) the Au surface was re-exposed after applying 3V.

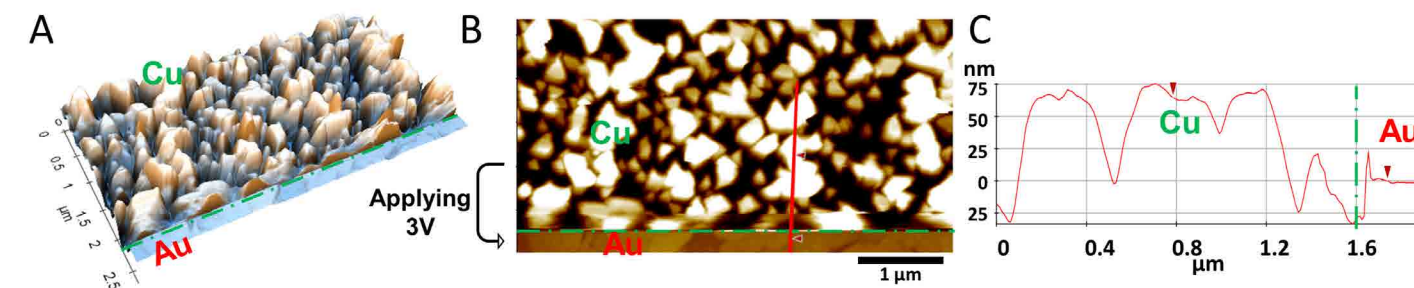


Figure 4. In situ 3D display (A) of the AFM image (B) acquired in 1 mM CuSO_4 showing bare Au surface (lower part) exposed after dissolution of electrochemically deposited copper clusters (upper part) at $E = 3$ V, $5 \mu\text{m} \times 2.6 \mu\text{m}$, vertical range 200 nm. The corresponding line cursor profile (C) quantifies the height difference between copper and gold regions.

The in situ dissolution of copper was also monitored with AFM. In the middle of the imaging, positive voltage was applied at the position of the horizontal green dashed line. Tall copper islands (up to 75 nm) dissolved, exposing the bare Au surface (Figure 4). This morphologic change in the middle of the image was clearly characterized via AFM. Likewise, one can also record the in situ deposition using AFM by shifting it to negative voltage.

Conclusion

The result of this study demonstrates that an advanced atomic force microscopy system with electrochemical cell can effectively measure electrochemical process in situ. It shows that a Park NX12 EC-AFM with Potentiostat can be set up easily and obtain data from electrochemical reactions in a controlled mechanism. The process of copper deposition is controlled by changing the applied voltage, and it is fully reversible. This experiment shows a lot of promise for

the study of nanoscale electrochemical reactions using Park EC-AFM.

References

- Vidu, R., and Hara, S., Surface alloying at the Cd|Au (100) interface in the upd region. *Electrochemical studies and in situ EC-AFM observation*. *Journal of Electroanalytical Chemistry* 475 (2) (1999) 171-180.
- Crow, D. R. (2017), *Principles and Applications of Electrochemistry*, Routledge.
- Reggente, M., Passeri, D., Rossi, M., Tamburri, E., and Terranova, M. L., In Electrochemical atomic force microscopy: In situ monitoring of electrochemical processes. *AIP Conference Proceedings*, AIP Publishing (2017) 020009.
- Huang, H. (2017). *Electrochemical Application and AFM Characterization of Nanocomposites: Focus on Interphase Properties* (PhD Dissertation). Stockholm. Retrieved from <http://urn.kb.se/resolve?urn=urn:nbn:se:kth:diva-203239>.
- Yamaguchi, Y., Shiota, M., Nakayama, Y., Hirai, N., and Hara, S., Combined in situ EC-AFM and CV measurement study on lead electrode for lead-acid batteries. *Journal of Power Sources* 93 (1-2) (2001) 104-111.
- Ban, I., Yamaguchi, Y., Nakayama, Y., Hirai, N., and Hara, S., In situ EC-AFM study of effect of lignin on performance of negative electrodes in lead-acid batteries. *Journal of Power Sources* 107 (2) (2002) 167-172.
- Vidu, R., Quinlan, F. T., and Stroeve, P., Use of in situ electrochemical atomic force microscopy (EC-AFM) to monitor cathode surface reaction in organic electrolyte. *Industrial & Engineering Chemistry Research* 41 (25) (2002) 6546-6554.
- Niu, L., Yin, Y., Guo, W., Lu, M., Qin, R., and Chen, S., Application of scanning electrochemical microscope in the study of corrosion of metals. *Journal of Materials Science* 44 (17) (2009) 4511-4521.
- Davoodi, A., Pan, J., Leygraf, C., and Norgren, S., In situ investigation of localized corrosion of aluminum alloys in chloride solution using integrated EC-AFM/SECM techniques. *Electrochemical and Solid State Letters* 8 (6) (2005) B21-B24.
- Rezaei, B., and Irannejad, N. (2019). Electrochemical detection techniques in biosensor applications. In Ali Ensafi (Ed.) *Electrochemical Biosensors* (pp 11-43).

NANO INFRARED (IR) PHOTO-INDUCED FORCE MICROSCOPY (PIFM):

A TECHNIQUE FOR NANOSCALE HYPERSPECTRAL MAPPING

Sung Park, Molecular Vista, San Jose, CA 95119

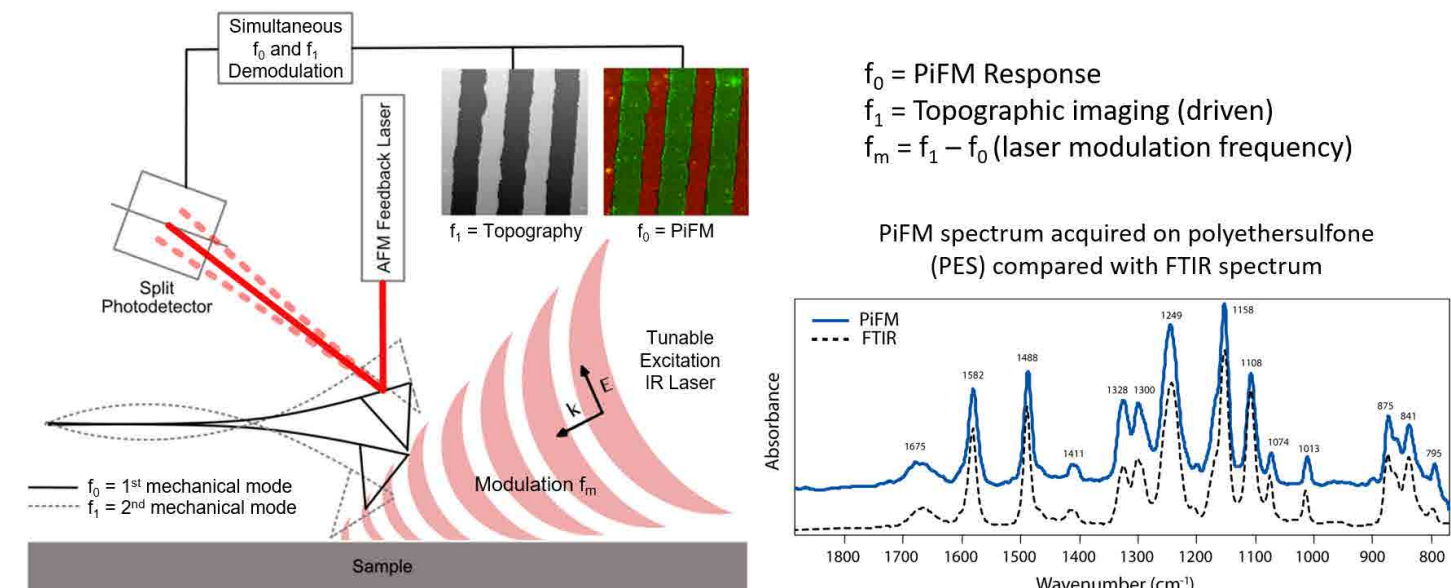
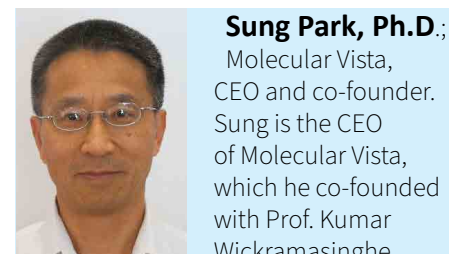


Figure 1. Schematic diagram of PiFM showing the AFM cantilever (two fundamental flexural mechanical modes at f_0 and f_1 are shown) and the external tunable IR laser used to excite the sample. Inset shows a FTIR spectrum and PiFM spectrum on polyethersulfone; the agreement between the two spectra are excellent even though FTIR and PiFM spectra originate from bulk and 10 nm region respectively.



Sung Park, Ph.D.;

Molecular Vista, CEO and co-founder. Sung is the CEO of Molecular Vista, which he co-founded with Prof. Kumar Wickramasinghe (UC Irvine, formerly of IBM) in 2011 to provide research and industrial tools for rapid and nanoscale imaging with chemical identification. Sung has over 25 years of experience of industrial R&D, engineering, marketing and sales, and operations. He co-founded Park Scientific Instruments (PSI), which was one of the first commercial companies to develop and sell scanning tunneling microscopes (STM) and atomic force microscopes (AFM). Prior to founding Park Scientific Instruments, he worked as a post-doc at IBM Watson Research Center. Sung earned his Ph.D. in Applied Physics from Stanford University and BA in Physics from Pomona College.

Introduction

Advances in nanotechnology have intensified the need for analytical tools that can chemically characterize newly synthesized nanomaterials. While electron microscopy (EM) techniques can identify atomic species through energy dispersive X-ray analysis, they offer little help for identification of molecular materials.[1] For identification of molecular species, well established optical spectroscopy (OS) techniques such as Raman and Fourier Transform Infrared (FTIR) are used; their spatial resolutions are governed by the diffraction limit, on the order of a micron, falling far short of the needs of the nanotechnology and nanomaterial researchers.[1] In order to overcome the diffraction limit of the OS techniques, various near-field techniques based on atomic force microscopy (AFM) have been developed. Techniques such as tip-enhanced Raman spectroscopy (TERS)[2-6] and scattering scanning near-

field optical microscopy (s-SNOM)[7-10] utilize an AFM tip to optically excite the sample just below the tip apex via a tip-enhanced near-field. A photon detector, placed in the far-field (far from the sample tip area), collects the emission from both the diffraction limited focal spot (far-field) and the near-field excited volume under the AFM tip. To selectively access the near field information, various methods are employed to suppress the far-field background signal in s-SNOM or greatly enhance the near-field signal in TERS. The suppression in s-SNOM and enhancement in TERS are both technically feasible but render the techniques more difficult to use. To overcome the difficulties associated with the convolution of near-field and far-field information, optical forces on the AFM tip can be measured directly. One such technique, photothermal induced resonance microscopy (PTIR)[11-15], measures thermal expansion due to optical absorption with an AFM tip in

contact with the sample. Although this technique is relatively straightforward to operate, thermal diffusion enlarges the effective detection region and compromises the spatial resolution.

Photo-induced Force Microscopy (PiFM)

In this article, we introduce infrared (IR) photo-induced force microscopy (PiFM) [16-22], which combines atomic force microscopy and IR spectroscopy (AFM-IR) to provide a technique for multi-modal nanoscale hyperspectral mapping, i.e., both IR spectroscopy and chemical mapping correlated with topography with sub-10 nm spatial resolution as shown in figure 1. IR PiFM relies on near-field excitation like other near-field microscopes. However, it is the only near-field microscope that acquires the sample's optical response by measuring the optically induced attractive force (total dipole-dipole force that consists of image dipole force and van der Waals mediated thermal expansion force) in the near-field while rejecting any competing far-field background signals.[22] To generate the photo-induced force (PiF), a widely tunable IR excitation laser, tuned at a specific wavenumber, is modulated at a frequency (f_m) to excite the first mechanical resonance, f_0 , of the AFM cantilever that is operated in non-contact mode with small dither amplitude (~ 1 nm) at the second mechanical resonance, f_1 . When f_m is set at the difference of the two mechanical resonances ($f_1 - f_0$), the standard topography (van der Waals force driven) and PiF signals can be acquired simultaneously by using two lockin amplifiers to demodulate the AFM force sensor signal (f_1 and f_0 will measure topography and IR absorption signal respectively). The PiF signal, measured as the amplitude of the cantilever oscillation at f_0 , will reflect the magnitude of IR absorption by the sample (this is true for most samples; see reference [22] for the exact nature of measured signal for different kinds of samples) at the excitation wavenumber. By sweeping the laser wavelength while recording the PiF signal, one can generate a PiFM spectrum, which shows excellent correlation with the bulk FTIR spectrum (see figure 1). The topography and PiF signals arise from the same point and allow perfect correspondence between IR absorption and topography.

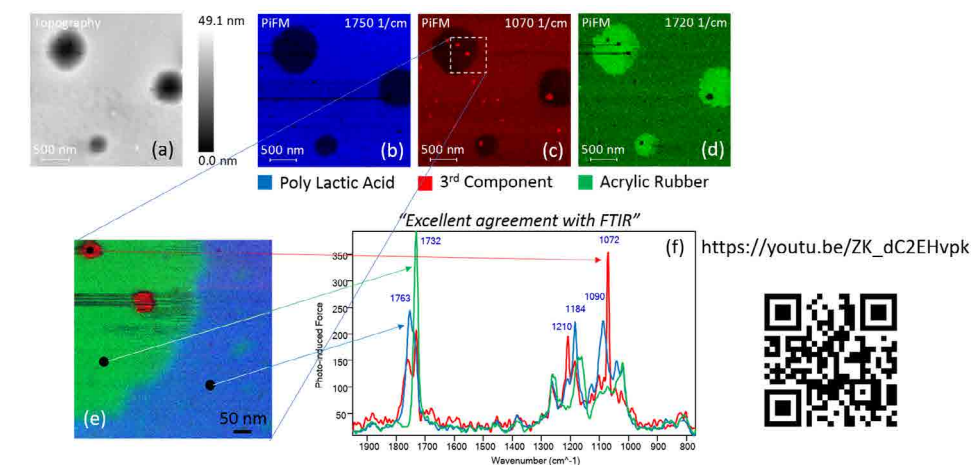


Figure 2. (a) Topography and PiFM images at (b) 1750 cm⁻¹, (c) 1070 cm⁻¹, and (d) 1720 cm⁻¹ for PLA, 3rd component, and ACM respectively. A zoomed in (e) composite image consisting of three PiFM images and (f) three spectra from locations shown in (e). QR code leads to a Youtube video showing acquisition of these data in real time.

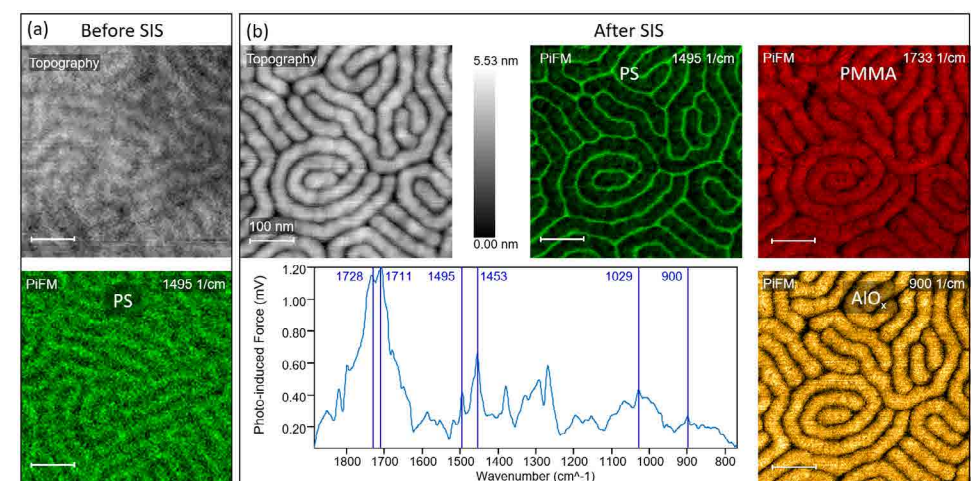


Figure 3. (a) Topography and PiFM image highlighting the PS block of PS-b-PMMA block copolymer with full pitch of 41 nm before SIS process. (b) Topography and PiFM images of PS, PMMA, and AlOx molecules acquired at 1495 cm⁻¹, 1733 cm⁻¹, and 900 cm⁻¹ respectively along with a PiFM spectrum after SIS process.

Applications

Figure 2 shows how PiFM can be used to study a polymer blend, in this case, of poly(lactic acid) (PLA)/acrylic rubber (ACM), which combines a biodegradable thermoplastic and a natural elastomer to create a usable and more eco-friendly material.[23] In practice, especially when the sample constituents are unknown, AFM topography (figure 2(a)) may be acquired first. Then a few PiF spectra can be acquired at unique features in topography, which will generate spectra that are like those seen in figure 2(f). Seeing that there are strong peaks at ~ 1730 cm⁻¹, the laser can be tuned to ~ 1730 cm⁻¹ (in this case, 1750 cm⁻¹) to acquire the AFM topography and PiFM image at 1750 cm⁻¹ (images 2(a) and

2(b)) concurrently. The process can be repeated to acquire PiFM images that show unique features and spectra associated with them. Different PiFM images can be artificially colored and then combined to form a chemical map as shown in figure 2(e) where three PiFM images at 1750, 1720, and 1070 cm⁻¹ are colored blue, green, and red to represent poly(lactic acid), acrylic rubber, and a third component respectively, and combined into one chemical map image. Note that three distinct spectra are acquired from three locations shown in figure 2(e) and displayed in figure 2(f); PiFM spectra can be reliably acquired from regions as small as ~ 10 nm in size. Use the QR code in figure 2 to see a video of how this sequence of data is acquired.

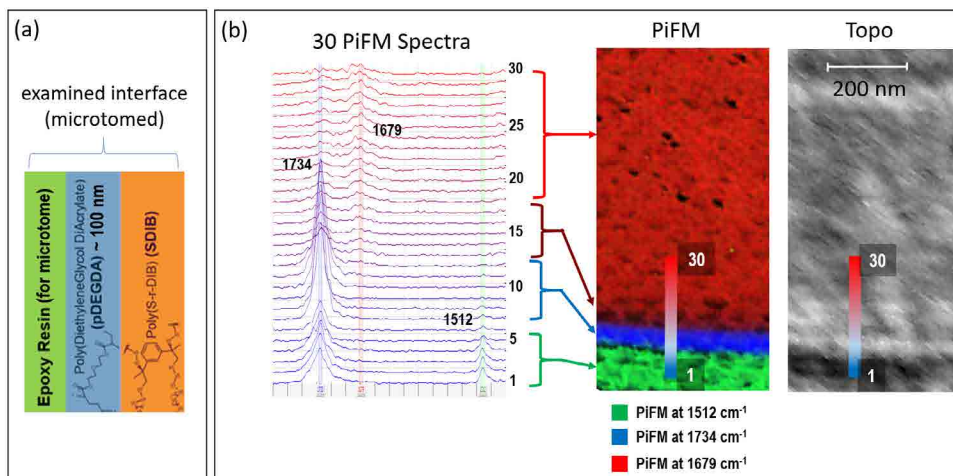


Figure 4. (a) Sample description of the polymer bi-layer cast in resin for cryo microtome. (b) Topography and a composite PiFM image (consisting of three PiFM images acquired at 1512 cm⁻¹, 1734 cm⁻¹, and 1679 cm⁻¹ to highlight resin, pDEGDA, and SDIB respectively) along with 30 spectra taken across the interface.

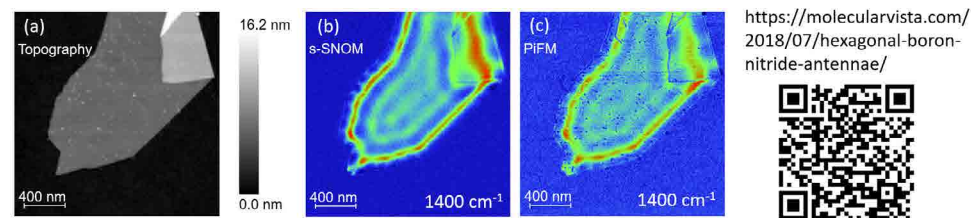


Figure 5. (a) Topography of a hBN flake concurrently imaged by (b) s-SNOM and (c) PiFM at 1400 cm⁻¹, both showing clear surface phonon polariton interference patterns.

Figure 3 shows an organic/inorganic composite system that was analyzed by PiFM. To generate a hard mask for etching for advanced lithography, aluminum oxide is selectively incorporated into PMMA block in a PS-b-PMMA block copolymer thin film through a process called sequential infiltration synthesis (SIS).²⁴ Figure 3(a) shows the topography and PiFM image of the PS block of the PS-b-PMMA with a full pitch of 41 nm before SIS process (500 nm x 500 nm, 128 x 128 pixels). Figure 3(b) shows the topography and PiFM images of PS, PMMA, and aluminum oxide along with a spectrum acquired at a random site of the sample after the SIS process (500 nm x 500 nm, 256 x 256 pixels). The spectrum shows the peaks associated with all three components given the small pitch. PiFM reveals that aluminum oxide selectively infiltrated only the PMMA block, causing a significant swelling of the PMMA block; after the SIS process, PS block has been squeezed to less than 10 nm in width.

PiFM can be used to analyze interfaces between different materials composing a multi-layer system by creating a cross-section of the sample. For thin films such as multi-layer polymers, the sample

can be embedded in a resin and cryo-microtomed in order to create a clean cut without surface contamination by the resin. For a crystalline sample such as silicon, it can be cleaved for analysis. Figure 4 shows the PiFM result obtained on the interface of poly(diethyleneglycol diacrylate) and poly(sulfur-r-diisopropenylbenzene), which are abbreviated as pDEGDA and SDIB. Figure 4(a) shows the three layers (resin, pDEGDA, and SDIB) that are exposed via cryo microtome. Of interest is to examine the extent of nanoscale mixing at the pDEGDA and SDIB interface. Given the thin pDEGDA layer (~ 100 nm), we used a mode called hyPIR (hyperspectral PiFM IR) where a PiFM spectrum was acquired at each pixel of the 128 x 128 image data (for 1 μm x 1 μm region). Even though each spectrum only took about 0.2 seconds, the whole image took about an hour to acquire. Once hyPIR data is acquired, much analysis can be derived from a single data set. Figures 4b(i) shows the topography of the cross-section while figure 4b(ii) is a composite of three PiFM images at 1512, 1734, and 1679 cm⁻¹ to highlight the resin, pDEGDA, and SDIB respectively. From the composite image, we can tell that (1) the interface between

resin (colored green) and pDEGDA (colored blue) is clean and abrupt and (2) the interface between pDEGDA and SDIB (colored red) consists of ~60 nm of strong pDEGDA signal and an interface region of ~60 nm where the pDEGDA signal gradually decreases and SDIB signal increases. Since the data has spectra associated with every pixel, we also looked at 30 spectra across the interface (each spectrum is about 10 nm from each other), which are shown in figure 4(b). The IR peaks used to highlight the components are highlighted by vertical bands. Looking at the spectra, we see that the resin peak at 1512 cm⁻¹ is greatly diminished from spectrum 4 to 5 (using the peak at 1734 cm⁻¹, the abrupt change is taken place from spectrum 6 to 7). The SDIB peak at 1679 cm⁻¹ seems to be at full strength around spectrum 18 when the pDEGDA peak at 1734 cm⁻¹ has dropped significantly from spectrum 12 to 13; the mixing between pDEGDA and SDIB takes place from spectrum 12 to 18 (~ 60 nm consistent with the composite image).

PiFM measures the total dipole-dipole attractive force that exists between the tip and the sample in the presence of an excitation light. Since IR PiFM measures the total attractive force, as opposed to only the repulsive force as in PTIR (which measures only the imaginary part of the complex polarizability), it can map both the molecular absorption as well as nanoscale surface plasmon and phonon polaritons making it a truly versatile and reliable near-field optical microscopy technique with the best spatial resolution. [22] Figure 5(a) shows a hexagonal boron nitride (hBN) film whose surface phonon polariton interference patterns have been widely measured by s-SNOM.[25-26] With Vista-IR system from Molecular Vista, both PiFM and s-SNOM measurements can be performed together; images 4(a), 4(b), and 4(c) are topography, s-SNOM, and PiFM images acquired concurrently. For this measurement, the signal-to-noise for PiFM is not quite as high as s-SNOM since the parameters were optimized for s-SNOM for concurrent acquisition; even so the agreement between the two measurement techniques is excellent. Use the QR code in figure 5 to see a video on the advantage of hyPIR imaging for characterizing resonant modes of artificial structures.

Conclusion

IR PiFM provides hyperspectral chemical analysis along with AFM at a scale (~ 5 nm spatial resolution) heretofore unattainable with any techniques on diverse samples including semiconductors, solar cell materials, plasmonics, organics, inorganics, pharmaceuticals, biological specimens (proteins, nucleotides, plants, tissues), 1D/2D materials, and geological specimens.

Acknowledgements

The author wishes to gratefully acknowledge the following collaborators for supplying the samples used in this study; PLA-ACM: Dr. Rudiger Berger from Max Planck Institute of Polymer; AlOx infiltrated into PS-b-PMMA: Dr. Ricardo Ruiz of HGST; pDEGDA-SDIB: Eui Tae Kim and Professor Kookheon Char of Seoul National University; hBN: Dr. Cian Bartlam of University of Manchester.

- 1] See <https://www.eag.com/techniques/> for a chart that compares existing analytical techniques. Not technique offers "chemical bonding/molecular/structural information" at length scale below about 200 nm.
- [2] R.M. Stöckle, Y.D. Suh, V. Deckert, and R. Zenobi, *Chem. Phys. Lett.* 318, 131 (2000).
- [3] N. Hayazawa, Y. Saito, and S. Kawata, *Appl. Phys. Lett.* 85, 6239 (2004).
- [4] A. Hertschuh, N. Anderson, and L. Novotny, *J. Microsc.* 210, 234 (2003).
- [5] S. Berweger, J.M. Atkin, R.L. Olmon, and M.B. Raschke, *J. Phys. Chem. Lett.* 1, 3427 (2010).
- [6] N. Jiang, E.T. Foley, J.M. Klingsporn, M.D. Sonntag, N.A. Valley, J.A. Dieringer, T. Seideman, G.C. Schatz, M.C. Hersam, and R.P. Van Duyne, *Nano Lett.* 12, 5061 (2012).
- [7] N. Ocelic, A. Huber, and R. Hillenbrand, *Appl. Phys. Lett.* 89, 101124 (2006).
- [8] M.B. Raschke and C. Lienau, *Appl. Phys. Lett.* 83, 5089 (2003).
- [9] A. Dazzi, R. Prazeres, F. Glotin, and J.M. Ortega, *Opt. Lett.* 30, 2388 (2005).
- [10] A. Dazzi, F. Glotin, and R. Carminati, *J. Appl. Phys.* 107, 124519 (2010).
- [11] A. Dazzi, C.B. Prater, Q. Hu, D.B. Chase, J.F. Rabolt, and C. Marcott, *Appl. Spectrosc.* 66, 1365 (2012).
- [12] F. Lu, M. Jin, and M.A. Belkin, *Nat. Photonics* 8, 307 (2014).
- [13] K. Kjoller, J.R. Felts, D. Cook, C.B. Prater, and W.P. King, *Nanotechnology* 21, 185705 (2010).
- [14] I. Rajapaksa, K. Uenal, and H.K. Wickramasinghe, *Appl. Phys. Lett.* 97, 073121 (2010).
- [15] A. Cvitkovic, N. Ocelic, and R. Hillenbrand, *Nano Lett.* 7, 3177 (2007).
- [16] Z. Fei, A.S. Rodin, G.O. Andreev, W. Bao, A.S. McLeod, M. Wagner, L.M. Zhang, Z. Zhao, M. Thieme, and G. Dominguez, *Nature* 487, 82 (2012).
- [17] D. Nowak, W. Morrison, H.K. Wickramasinghe, J. Jahng, E. Potma, L. Wan, R. Ruiz, T.R. Albrecht, K. Schmidt, J. Frommer, D.P. Sanders, and S. Park, *Sci. Adv.* 2, e1501571 (2016).
- [18] J. Jahng, J. Brocius, D.A. Fishman, F. Huang, X. Li, V.A. Tamma, H.K. Wickramasinghe, and E.O. Potma, *Phys. Rev. B* 90, 155417 (2014).
- [19] J. Jahng, J. Brocius, D.A. Fishman, S. Yampolsky, D. Nowak, F. Huang, V.A. Apkarian, H.K. Wickramasinghe, and E.O. Potma, *Appl. Phys. Lett.* 106, 083113 (2015).
- [20] B. Kim, J. Jahng, R.M. Khan, S. Park, and E.O. Potma, *Phys. Rev. B* 95, 075440 (2017).
- [21] J. Jahng, E.O. Potma, and E.S. Lee, *Anal. Chem.* 90, 11054 (2018).
- [22] J. Jahng, E.O. Potma, and E.S. Lee, *PNAS*, 116 (52), 26359 (2019).
- [23] M. Hesami and A. Jalali-Arani, *J. Appl. Polym. Sci.*, 134, 45499 (2017).
- [24] R. Ruiz, L. Wan, J. Lille, K.C. Patel, E. Dobisz, D.E. Johnston, K. Kisslinger, and C.T. Black, *J. Vac. Sci. Technol. B* 30(6), 06F202-1 (2012).
- [25] S. Dai, Z. Fei, Q. Ma, A. S. Rodin, M. Wagner, A. S. McLeod, M. K. Liu, W. Gannett, W. Regan, K. Watanabe, T. Taniguchi, M. Thieme, G. Dominguez, A. H. Castro Neto, A. Zettl, F. Keilmann, P. Jarillo-Herrero, M. M. Fogler, D. N. Basov, *Science* 343, 1125 (2014).
- [26] M. Tamagnone, A. Ambrosio, K. Chaudhary, L.A. Jauregui, P. Kim, W.L. Wilson, F. Capasso, *Sci. Adv.* 4: eaat7189 (2018).

INDUSTRY NEWS: PARK SYSTEMS COMPLETES EQUITY INVESTMENT IN MOLECULAR VISTA



Molecular Vista develops and sells a specialized AFM instrument called VistaScope with Infrared Photo induced Force Microscopy (IR PiFM), which provides nanoscale imaging & spectroscopy.

Park Systems Corp. world-leading manufacturer of Atomic Force Microscopes (AFM), announced today it has made an equity investment in Molecular Vista (www.molecularvista.com), based in San Jose, CA. Molecular Vista produces AFM tools to probe and understand matter at the molecular level through quantitative visualization using Infrared Photo-induced Force Microscopy (IR PiFM).

PiFM is a combination of AFM and IR spectroscopy in a single instrument that acquires both topography and chemical signatures at the nanometer scale and is universally applicable to a wide range of organic and inorganic materials.

"We believe Molecular Vista's exclusive technology places them at the forefront of one of the fastest-growing segments of the AFM industry," comments Dr. Sang-il Park, CEO Park Systems. "Sung Park and the talented management team at Molecular Vista have created a cutting-edge company with an exciting future, and we are thrilled to become part of it."

AFM provides nanoscale topographic images and various other measurements including mechanical, electrical, and other physical characteristics of a sample. Now, with the addition of PiFM technology, it can provide researchers with chemical and molecular composition information combined with the nano physical data.

"The Park Systems investment will help us significantly expand our technology driven IR PiFM platform, filling a critical void in nanoscale molecular and chemical analysis," states Sung Park, CEO of Molecular Vista. "We are honored that Park Systems, a leader in AFM since its inception, has become an equity partner."

About Park Systems

Park Systems is the fastest growing and world-leading manufacturer of atomic force microscopy (AFM) systems, with a complete range of products for researchers and engineers in the chemistry, materials, physics, life sciences, semiconductor and data storage industries. Park Systems is a publicly traded corporation on the Korea Stock Exchange (KOSDAQ) with corporate headquarters in Suwon, Korea, and regional headquarters in Santa Clara, California, USA, Mannheim, Germany, Beijing, China, Tokyo, Japan, Singapore, and Mexico City, Mexico. To learn more about Park Systems, please visit www.parksystems.com.

Park Systems AFM - Highest Resolution, Accuracy and Ease of Use Brilliantly Combined

Park Systems creates the world's most accurate line of nanoscale microscopy and metrology tools for research and industrial applications. Our innovation features, such as True-Non Contact™ mode and cutting-edge automation, set our products apart from the competition and make Park Systems AFMs the easiest to use and most advanced AFMs available.

To find out more, please email us at inquiry@parksystems.com or visit us at www.parksystems.com

General AFMs

Park Systems provides a range of popular AFMs for general research and industrial applications. Designed to be extremely versatile while still providing the accuracy and functionality necessary to do high quality work, our line of general AFMs offer researchers and engineers alike the ability to get extremely accurate results quickly and easily.

Applications:

- Biological Science
- Materials Science
- Failure Analysis
- Semiconductor Analysis
- Hard Disk Media Analysis

Small sample AFM



Park XE7

True research-grade AFM for the practical budget



Park NX10

The world's most accurate easy-to-use research AFM



Park NX-Hivac

The most advanced high vacuum AFM for failure analysis and sensitive materials research

Large sample AFM



Park XE15

Capable, adaptable, and affordable-the best value large sample AFM



Park NX20

Power, versatility, ease of use, brilliantly combined for large sample AFM



Park NX20 300mm

The leading automated nanometrology tool for 300 mm wafer measurement and analysis

Bio and Chemical

Biological research is one of the fastest growing fields of the 20th century. Park AFMs have played critical roles in this sector, giving researchers the tools they need to develop novel insights into the vast and complicated processes and structures of biology.



Park NX10 SICM

Cutting-edge nanoscale imaging in aqueous environments



Park NX12-Bio

Three compelling nanoscale microscopies in one innovative platform



Park NX12

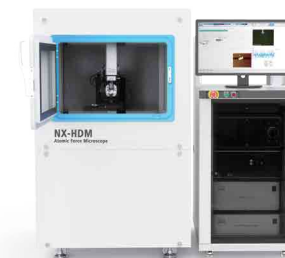
The most versatile AFM for analytical and electrochemistry

Industrial AFMs

Park Systems is dedicated not just to advancing research, but industry as well. That's why our designers have worked to build a line of the most effective AFMs for FA engineers and industrial applications. Allowing users to take highly accurate measurements and complete their work more quickly, these tools can improve efficiency in the workplace and reduce errors, leading to a more profitable, more consistent development and production process.

Applications:

- Failure Analysis
- Semiconductor Analysis
- Hard Disk Media Analysis



Park NX-HDM

The most innovative AFM for automated defect review and surface roughness measurement



Park NX-PTR

Fully automated AFM for accurate inline metrology of hard disk head sliders



Park NX-Wafer

Low noise, high throughput atomic force profiler with automatic defect review



Park NX-3DM

Innovation and efficiency for 3D metrology

DETECTION OF MAGNETIZATION
REVERSAL IN MAGNETIC PATTERNED
ARRAY USING MAGNETIC FORCEPark
SYSTEMS

John Paul Pineda, Byong Kim, and Keibock Lee, Park Systems Inc., Santa Clara, CA, USA

Abstract

Magnetization reversal plays a major role in designing the switching mechanisms of magnetic nanostructures in a high density storage device. In this study, magnetization reversal in a magnetic patterned array sample was successfully investigated using an atomic force microscopy (AFM) system via magnetic force microscopy (MFM). The magnetic property and topography data of a sample surface were obtained simultaneously and the data shows that the two signals are well separated by the two-pass scanning method. The MFM images demonstrate that a majority of the circular dot domain structures with 148 nm width on the sample surface experienced a magnetization reversal during the scan with a few domains remaining in their original state. Some of the circular dots that experienced a magnetization reversal switched their magnetization easily, while others switched gradually as the magnetic field between the tip and the sample changes over time. A single defect was also observed in the images of the acquired data. The results sum up that the technique described in this study can provide a reliable data in understanding the magnetization behavior and can be used in defect identification of a magnetic sample.

Introduction

Magnetic storage is vital to the digital era, and is implemented in a wide variety of devices including computers, cell phones, data servers, and others. The ability of magnetic storage devices to inexpensively store large amounts of information in a small area makes it attractive compared with other high-density storage technologies [1]. Maintaining a high signal to noise ratio (SNR) has become a great challenge in high density recording. One of the most effective methods for achieving an adequate SNR involves storing the data in a magnetic patterned array. In this method, the data are stored in lithographically defined magnetic patterns in the form of magnetic domains with each domain representing a single data

bit which can be either a 1 or a 0 bit. The magnetic properties of the nanostructures such as domain magnetization, shape, size, array spacing, etc. can greatly affect the performance of the magnetic storage device. Thus, a technique that can measure these characteristics and investigate samples with nanoscale features must be utilized in evaluating device reliability. There are several methods that can be used in investigating and monitoring magnetic domains. Examples include Photo Electron Emission Microscopy (PEEM), Scanning Electron Microscopy (SEM), X-ray Magnetic Circular Dichroism (XMCD), Kerr Effect Microscopy, among others [2, 3, 4, 5]. However, some of these methods do not provide high spatial resolution; while others have tedious sample preparation requirements, are destructive, or do not operate in ambient conditions. For these reasons, Magnetic Force Microscopy (MFM) was developed to overcome such shortcomings. In addition, the integration of the two techniques enables the user to acquire both topography and magnetic property data simultaneously without changing the sample or tip. To this end, MFM was used to investigate a magnetic patterned array and the data shows that this technique is an effective method for the magnetic properties characterization of magnetic storage devices.

Experimental

A magnetic patterned array sample was investigated using a Park NX10 Atomic Force Microscopy (AFM) system. The magnetic properties of the sample were characterized under ambient air conditions using MFM mode. A cantilever with a tip coated with a magnetic material (Nanosensors, PPP-MFMR) was magnetized prior to imaging and used in the entire experiment. A non-magnetic sample holder was also utilized to obtain an optimum measurement. The MFM measurements were performed using the conventional non-contact two-pass scanning method (see Figure 1). Four consecutive images were acquired at the

same position at 4 minute intervals to observe the magnetic domain variation over time.

In MFM mode, there are two interaction forces between the magnetized tip and the magnetic sample: the Van der Waals force and magnetic force. The van der Waals force is harnessed to generate the sample's surface topography while the magnetic force between the magnetized tip and magnetic sample generates data for the sample's magnetic properties. The obtained cantilever oscillation signal contains both sets of information; therefore, a method that can completely separate these signals is the key to successful imaging. One such method introduced to accomplish this task is two-pass scanning. In this method, the topography data is obtained in the first scan while the MFM data is obtained in the second scan. The tip is lifted during the second scan in the height where the only change in force affecting the cantilever oscillation signal is the change of the magnetic force as shown in Figure 1 [6]. In this experiment, the optimum value of tip-sample distance chosen to get a reliable MFM image is 50 nm. A lock-in amplifier which is embedded in the AFM system is used to analyze the tip motion caused by the van der Waals force in the first scan and magnetic force in the second scan. In MFM mode, the domain structures and polarity are detected by analyzing the changes in the cantilever's oscillation frequency caused by the magnetic field. The magnitude of the change in oscillation frequency is proportional to the magnetic field intensity. During scanning, the tip is either attracted toward or repulsed from the sample surface depending on the domain magnetization of the sample.

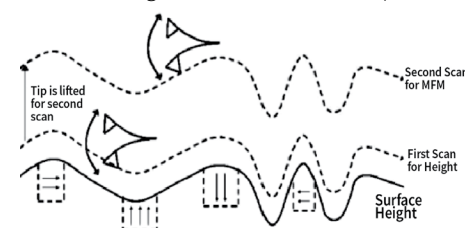


Figure 1. Two-pass scanning method of MFM mode.

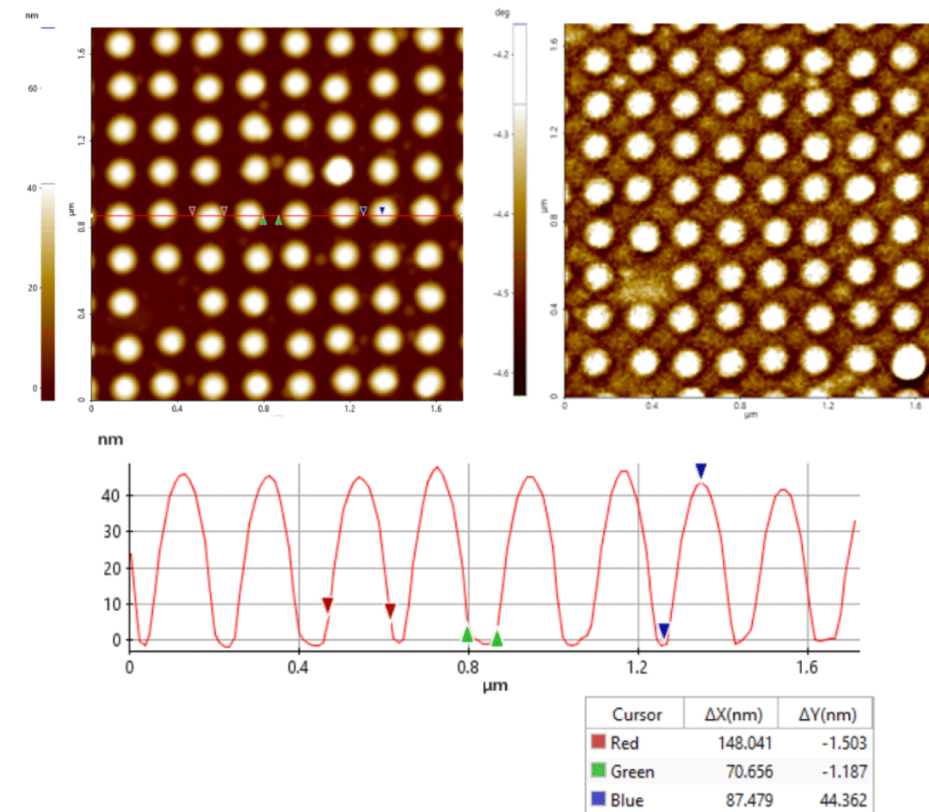


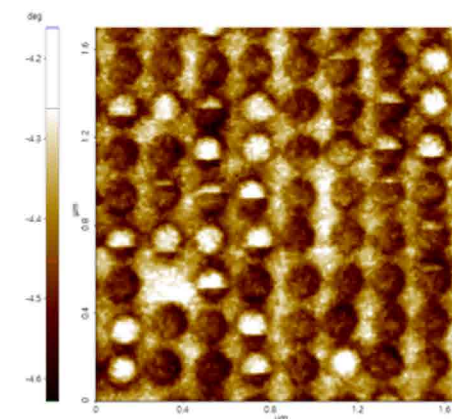
Figure 2. Topography (top-left) and MFM (top-right) data from the magnetic sample. Line profile of AFM topography (Red: circular dot diameter, Green: array spacing, Blue: circular dot height).

Results and Discussion

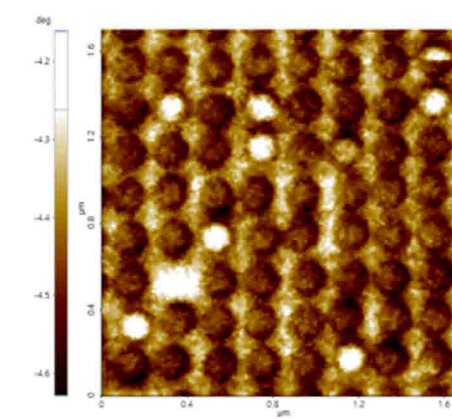
The topography data obtained in this experiment shows that a lattice structure with circular dots was successfully fabricated but no significant information related to its magnetic domain is provided. In contrast, the magnetic property data acquired in MFM measurements shows the magnetic domain structure and magnetization, but no significant information related to physical structure of the sample. The domain structure observed in MFM data of this sample is similar to the physical structure observed

in topography data, which is a patterned array consisting of circular dots. The data acquired in this experiment were all analyzed using XEI software developed by Park Systems. Figure 2 shows the topography and MFM measurement of the magnetic patterned array sample acquired at the first time point. The topography data shows a clear image of a well-defined lattice structure. The line profile that was generated by the XEI software in Figure 2 provides the geometrical information of the lattice structure. The data shows that the diameter of each circular region is approximately 148 nm in diameter (Figure

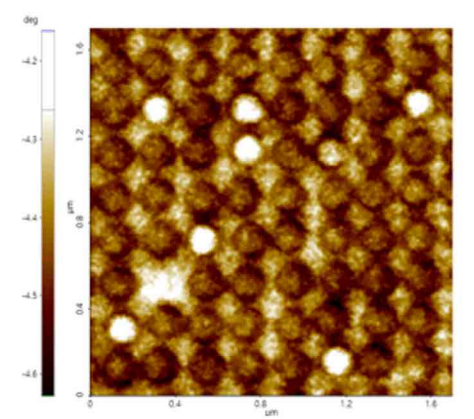
a.) MFM 4 minutes after magnetization



b.) MFM 8 minutes after magnetization



c.) MFM 12 minutes after magnetization

Figure 3. MFM data at a.) 4 minutes b.) 8 minutes and c.) 12 minutes following magnetization. Scan size: 1.7 μm x 1.7 μm .

2, red arrows) and 44 nm in height (Figure 2, blue arrows). The array spacing for the circular regions is approximately 71 nm (Figure 2, green arrows). The MFM image shows that the domain structures are also circular and all are bright in color. The contrast of the circular dots correlates to the domain magnetization. In this experiment, the bright color implies that the magnetic dipole points in an upward direction normal to the sample surface while a dark color implies a magnetization pointing in the downward direction. Thus, the MFM image demonstrates that the lattice structure at the initial time point is composed of a circular pattern in a magnetic single-domain state that are pointing in an upward direction.

Figure 3 shows the MFM measurements acquired every 4 minutes. Based on the color of the circular regions, Figure 3a shows the majority of the circular regions have completely switched magnetization polarization, while some have either partially switched or had no change. The partially switched domains represent a magnetic multi-domain state while the domain that experienced a complete magnetization reversal and those that remained on their original magnetization represents a magnetic single-domain state [7]. From this interpretation, the lattice after 4 minutes is comprised predominantly of single-domain states with a few multi-domain states. By monitoring the individual domains over time, it is observed that most of the single-domain states experienced a complete magnetization reversal. The same interpretation can be made in Figure 3b, however, most of the partially switched domains at the second time point have completely switched their magnetization by the third time point. At the final time

point, Figure 3c shows the structure is composed of circular dots that are all in a single-domain state. The majority of these single-domain states are the ones that experienced a complete magnetization reversal pointing in a downward direction. The remaining circular dots with bright colors are the ones that remained at their initial magnetization during the entire process. The absence of the switch in magnetization of these domains could be due to surface non-uniformity [8]. It is speculated that the magnetization reversal is caused by the changed in the magnetic field between the tip and the sample over time. A surface irregularity on the lattice structure was also observed on the lower left sides of all the images. This irregularity is speculated to be a single defect that was acquired during the fabrication process [9, 10]. Such individual defects could greatly affect the magnetic reversal properties of the sample [10].

Conclusions

The lattice structure of the magnetic patterned array was successfully characterized by the Park NX10 AFM using MFM mode imaging. The topography data revealed that the lattice structure is composed of circular regions with a diameter of 148 nm and height of 44

nm. The MFM data shows that a majority of the magnetic domains experienced a magnetization reversal during the scan with a few domains remaining in their original state as the magnetic field between the tip and the sample changes over time. A surface irregularity was also observed on the images speculated to be a single defect consisting of a region that does not exhibit magnetic properties likely created during the fabrication process. Characterization of magnetization reversal is significant in designing the switching mechanisms of magnetic nanostructures. A well designed switching mechanism is important especially in writing the information in a bit cell. Failure of inversion of a single bit during writing will lead to data loss or corruption. Overall, the technique described in this study could be used in the investigation of magnetization reversal behavior and defect identification of high-density magnetic storage devices.

References

- [1] Z. Bandic, et al., Advances in Magnetic Data Storage Technologies. Scanning the issue
- [2] K. Koike, et al., Scanning Electron Microscope Observation of Magnetic Domains Using Spin-Polarized Secondary Electrons. Japanese Journal of Applied Physics, Volume 23, Part 2, Num. 3.

- [3] P. Kasiraj, et al., Magnetic domain imaging with a scanning Kerr effect microscope. IEEE Transactions on Magnetics, Volume: 22, Issue: 5, Sep 1986.
- [4] C. Schneider, et al., Investigating surface magnetism by means of photoexcitation electron emission microscopy. Reports on Progress in Physics, Volume 65, Number 12.
- [5] P. Fischer, et al., Imaging of magnetic domains with the X-ray microscope at BESSY using X-ray magnetic circular dichroism. Zeitschrift für Physik B Condensed Matter, December 1997, Volume 101, Issue 3, pp 313–316.
- [6] Park MFM Technique: [http://www.parkafm.com/images/spmmodes/magnetic/Magnetic-Force-Microscopy-\(MFM\).pdf](http://www.parkafm.com/images/spmmodes/magnetic/Magnetic-Force-Microscopy-(MFM).pdf).
- [7] P. Krone, et al., Investigation of the magnetization reversal of a magnetic dot array of Co/Pt multilayers. Journal of Nanoparticle Research, November 2011, Volume 13, Issue 11, pp 5587–5593
- [8] A. Fraerman, et al., Observation of MFM tip induced remagnetization effects in elliptical ferromagnetic nanoparticles. Institute for Physics of Microstructures RAS, Nizhny Novgorod, Russia
- [9] A. Manzin, et al., Influence of lattice defects on the ferromagnetic resonance behaviour of 2D magnonic crystals. Scientific Reports 6, Article number: 22004
- [10] X. Hu, et al., The influence of individual lattice defects on the domain structure in magnetic antidot lattices.

FEATURED ARTICLE



Corresponding author:
Ana Maria Zaske PhD
 Internal Medicine,
 Cardiology Division,
 University of Texas Health Science
 Center at Houston. 1881 East Rd,
 Houston TX, 77054, USA. Email:
Ana.M.Zaske@uth.tmc.edu

Biography

Ana-Maria Zaske graduated in 2001 with a PhD from the University of Manchester Institute of Science and Technology in the UK, where she specialized in high resolution Atomic Force Microscopy (AFM) to resolve bio-enzymatic processes. She used AFM as a Research Associate in the laboratory of Molecular and Cellular Neurobiology, at the UNAM Mexico, to characterize membrane receptors in follicular cells. In 2004 she did her post-doctoral studies at North Carolina State University. In 2008, she joined the University of Texas Health Science Center at Houston, and later she became the manager of the IM Bioscope 2 - UT core facility. Over the course of her career, Dr. Zaske has gained relevant expertise in the principles and applications of AFM in the biological and medical field. She visualizes the AFM technique as a revolutionary tool to explore the nano-world.

USING ATOMIC FORCE MICROSCOPY IN MEDICAL RESEARCH

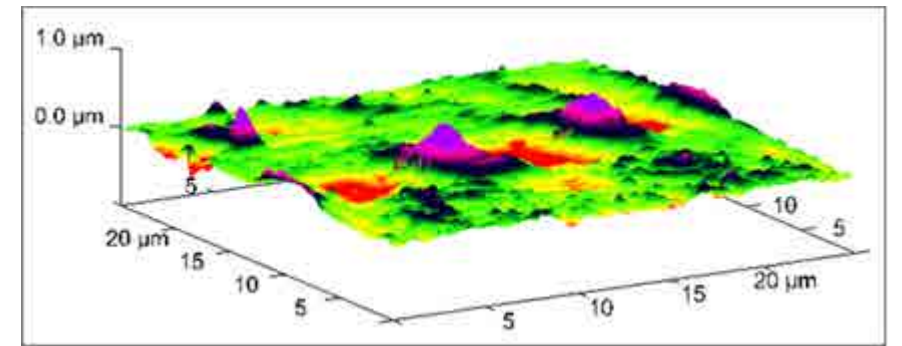


Figure 1. Liposome endocytosis occurring at 60 min of incubation in HCAEC's. 3D AFM micrograph obtained at 25 µm (x-y) illustrating the engulfment of liposomes conjugated with gold nanoparticles during membrane internalization [1].

Nano-biotechnologies represent an unprecedented recent advance that may revolutionize many areas of medicine and biology. We are now able to evaluate the effects of a treatment in cancer cells, analyze the efficiency of skin healing or just simply observe DNA structures, all at the nano-metric scale. One of the major advances, in the nano-technology field, was the development of the Atomic Force Microscope (AFM) in 1982, as a modification of the first scanning tunneling microscope created by Gerd Binnig. Binnig is the German physicist that won the Nobel Prize in Physics along with Heinrich Rohrer in 1986 for their invention.

The AFM is a nano-technique based on sensing. Such as "feeling" or "touching" the sample surface with a very small flexible probe, while a feedback loop regulates the gap distance between the sample and the probe. The AFM imaging is, therefore, a mechanical process based on attractive and repulsive forces between the sample surface and the probe, giving resolutions to the nanometer level.

Several models of Atomic Force Microscopes have been specifically designed to address the needs of biological and medical investigations. The mission at our AFM core facility located in the University of Texas Health Science Center at Houston, is to explore all meaningful ways to assess experimental

trials to mitigate diseases using Atomic Force Microscopy. The BioScope™ II microscope at our core, has been engineered to facilitate advanced life science research such as imaging, probing and manipulating biological systems. All three axes (X, Y, and Z) of the instrument are equipped with high-resolution capacitive sensors to allow imaging at the nanoscale and operating in liquids. It has the ability to analyze samples in the natural state in dry conditions or 'in-vitro', immersed in biological solutions. The instrument also has an unprecedented compatibility with optical microscopy to facilitate the localization of the areas of interest.

Cell cultures are widely used to mimic biological conditions where physiological reactions take place. The effects of a treatment or disease can be assessed analyzing the changes in structure and elasticity of living cells using AFM. The interaction of biomolecules with various types of controlled nano-particles is also becoming highly important for many biological and biomedical applications. In combination with fluorescence microscopy, AFM can identify biomolecules based in fluorescence labeling and topography imaging. In addition, non-cellular structures can also be imaged. We can now determine the micromechanical properties of both biological and non-biological materials. Additionally, this technology requires

2020 NanoScientific Forum Europe

Scanning Probe Microscopy (SPM)

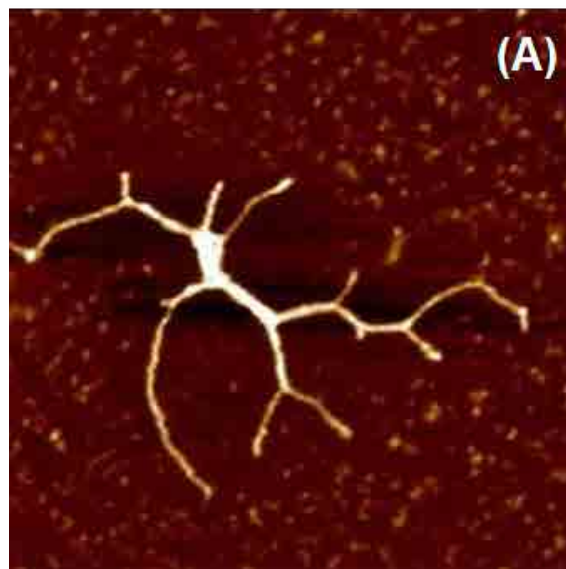
23 - 25 September 2020

Trinity College Dublin

Dublin, Ireland

SPONSORED BY

parksystems.com



Macro-molecules

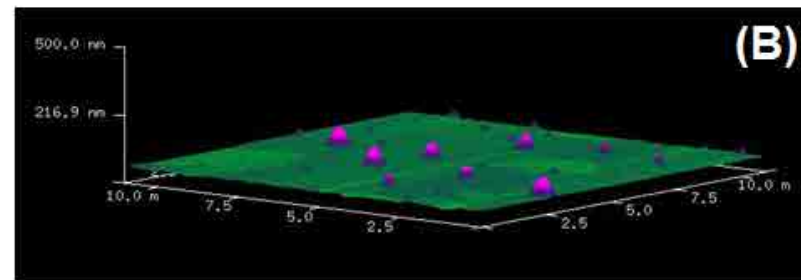


Figure 2. (A) AFM image of a full length myosin protein visualized at RT on mica. Scan to 2 μm (x-y) using tapping mode in air. (B) 3D AFM micrograph of DPPC liposomes deposited on mica.

minimal sample preparation procedures, which enhances its popularity in the field.

Some of the AFM applications that we routinely use in our laboratory include:

- Topographical imaging of samples in air or liquid environments
- High-resolution imaging at the nano-metric scale
- Time-lapse experiments that show real-time changes in sample morphology or structure
- Nano-probing of samples to measure molecular interactive forces
- Studies of local micromechanical properties (elasticity, stiffness, adhesion, roughness)
- Data analysis for determination of homogeneity of samples, size distribution, position, force volume mapping and 3D imaging.

Surface processes such as endocytosis/exocytosis, interactions between cells and other surfaces, the dynamic reorganization of the cytoskeleton, or analysis of surface configurations are between the topics extensively studied using the AFM technique. An area of major interest, among our researchers, is to determine the stiffness of a sample (Elastic Modulus). By calculating the Young's modulus on the surface, we

can evaluate the effects of several physiological processes by measuring the elastic response on cells and tissues. As per example, the elasticity of the cell membrane can vary between cell types as a function of growth, differentiation, disease or treatment.

Over the years, we have gained relevant experience to apply the fundamentals of AFM to medical research. We initiated studying the internalization mechanism and effects of nanovectors in 'in-vitro' cells [1]. We determined the time it takes for the cell to uptake gold labelled liposomes for medical applications. We excitedly captured the moment during liposome membrane internalization as seen in Figure 1. We also studied the cell intake of a multi-delivery system consisting of porous silicon microparticles (SiMPs) loaded with one or more types of second-stage nanoparticles. Each level of complexity presents an opportunity for overcoming physiological barriers, such as enzymatic degradation, vascular transport, crossing endothelium, and bypassing molecular efflux pumps [2]. We have also used AFM to determine the structural properties of several other nanovectors such as exosomes, liposomes, microvesicles and chitosan nanoparticles with therapeutic properties (Figure 2).

I have had the opportunity to participate in several multidisciplinary projects at UT-Health. For example, we studied the effects of frozen plasma as a resuscitative agent with Kozar's group [3]. We determined that plasma based resuscitation, preserved endothelial

integrity in an in-vitro model of shock. In these studies, shock (or endothelial injury) disrupted junctional integrity and increased permeability in cell cultures. Fresh frozen plasma restored the endothelial integrity and reduced syndecan-1 shedding after hemorrhagic shock. In a different project, we monitored dynamic morphological changes of human platelets in real-time using AFM. We noticed that platelet formation is independent of the interaction between fibrinogen and the platelet integrin $\text{aIIb}\beta_3$. However, platelets were very sensitive to agonist-induced micro-vesiculation [4]. In a most recent work with Dr. Yong Zhou [5], AFM was used to determine roughness of cell plasma membranes to quantify several modulations of the lipid-anchored K-Ras expression, which is known to regulate proliferation in cancer cells.

New insights have developed, in the AFM field, to determine the elastic properties of biological materials. We routinely estimate the Young's Modulus of cell membranes, fresh tissues and other biological samples, to help to understand the mechanisms of several physiological processes, such as differentiation, growth, drug treatment, metastasis and disease [6], [7]. Additionally, it is possible to map the distribution of elastic responses on the sample surface (Force Volume maps) by combining force curve measurements with topographic imaging as shown in Figure 3 with tissue samples.

The unique properties of the AFM offer unlimited applications in medical research.

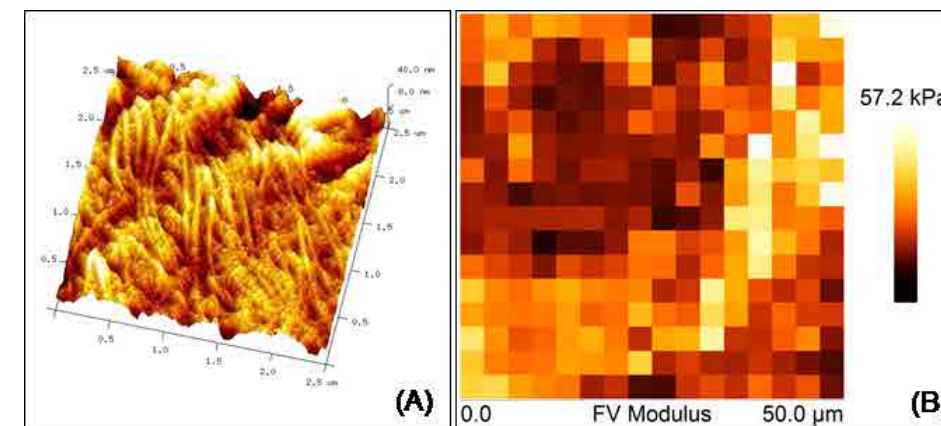


Figure 3. Elastic properties associated with skin healing. Color-coded force maps were generated over skin biopsies to determine collagen deposition as a promoter of wound healing in transgenic mice. (A) AFM micrograph obtained at 2.5 μm (x-y) showing topography of a skin wound. (B) Force Volume map of a 50 μm (x-y) scan of the same skin area.

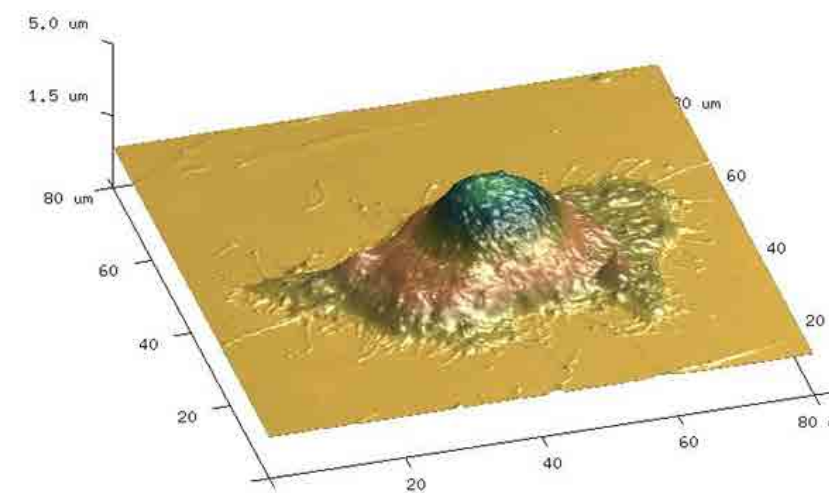


Figure 4. Studies on impact of sucrose as a modulator on cell proliferation and death. Atomic force micrograph of HeLa cells showing surface topography for volume measurements. Cell volume was calculated using the bearing analysis application and using contact mode operated in liquid [8].

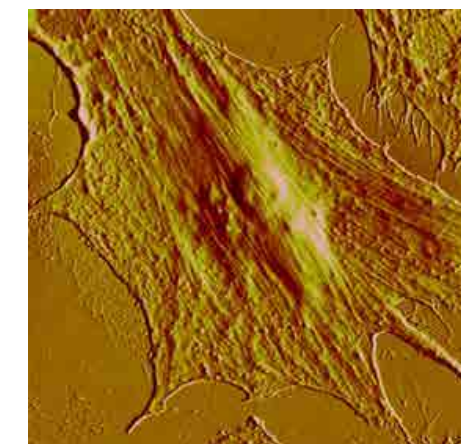


Figure 5. AFM image of a HUVEC (human umbilical vein endothelial cell) expressing E-selectin and incubated with ESTA-1 aptamer nano-beads after fixation with 4% formaldehyde. Image acquired in phosphate saline solution 1X.

It can provide valuable insights about the mechanisms of a disease, and assess a successful treatment pathway for its cure.

References

1. ZASKE, ANA-MARIA; DELIA DANILA; MICHAEL C. QUEEN; EVA GOLUNSKI; JODIE L. CONYERS (2013). "Biological Atomic Force Microscopy for Imaging Gold-Labeled Liposomes on Human Coronary Artery Endothelial Cells". *Journal of Pharmaceutics*, vol. 2013, Article ID 875906, 8 pages, DOI:10.1155/2013/875906.
2. SERDA, RITA E.; AARON MACK; MERLYN PULIKKATHARA; ANA-MARIA ZASKE; CIRO CHIAPPINI; JEAN R. FAKHOURY; DOUGLAS WEBB; BIANA GODIN; JODIE L. CONYERS; XUE W. LIU; JAMES A. BANKSON; MAURO FERRARI (2010). "Cellular association and assembly of a multi-stage delivery system". *Small [cover]* 6 (12): 1329-1340.
3. HAYWOOD-WATSON, RICKY; JOHN B. HOLCOMB; ERNEST A. GONZALEZ; ZHANGLONG PENG; SHIBANI PATI; PYONG WOO PARK; WEIWEI WANG; ANA MARIA ZASKE; TYLER MENGE; ROSEMARY A. KOZAR (2011). "Modulation of Syndecan-1 Shedding after Hemorrhagic Shock and Resuscitation". *PLoS ONE* 6:8, 1-10, e23530, DOI:10.1371/journal.pone.0023530.
4. ZHANG, YANJUN; XIAO LIU; LI LIU; ANA-MARIA ZASKE; ZHOU ZHOU; YUANYUAN FU; XI YANG; JODIE L. CONYERS; JING-FEI DONG; JIANNING ZHANG (2013). "Contact and Agonist Regulated Microvesiculation of human platelets". *Thrombosis and Haemostasis*, 2013; 110 (2):331-339.
5. HONG LIANG, HUANWEN MU, FRANTZ JEAN-FRANCOIS, BINDU LAKSHMAN, SUPARNA SARKAR-BANERJEE, YINYIN ZHUANG, YONGPENG ZENG, WEIBO GAO, ANA MARIA ZASKE, DWIGHT NISSLEY, ALEMAYEHU GORFE, WENTING ZHAO, and YONG ZHOU (2019). "Membrane curvature sensing of the lipid-anchored K-Ras small GTPase". *Life Science Alliance* (2019) DOI: <https://doi.org/10.26508/lsa.201900343> vol 2 / no 4 / e201900343.
6. LEE, SEI-YOUNG; ANA-MARIA ZASKE; TOMMASO NOVELLINO; DELIA DANILA; MAURO FERRARI; JODIE CONYERS; PAOLO DECUZZI (2011). "Probing the mechanical properties of TNF- α stimulated endothelial cell with atomic force microscopy". *International Journal of Nanomedicine* 6: 179-195.
7. HONG JIA, JAGADEESH JANJANAM, SHARON C. WU, RUIZHAN WANG, GLENDIN PANO, MARINA CELESTINE, OPHELIE MARTINOT, HANNAH BREEZE-JONES, GEORGIA CLAYTON, CECILE GARCIN, ABBAS SHIRINIFARD, ANA MARIA ZASKE, DAVID FINKELSTEIN, MYRIAM LABELLE (2019). "The tumor cell-secreted matricellular protein WISP1 drives pro-metastatic collagen linearization". *The EMBO Journal* (2019) E101302. DOI: 10.15252/EMBJ.2018101302.
8. PULIKKATHARA, MERLYN; COLETTE MARK; NATASHA KUMAR; ANA MARIA ZASKE; RITA E. SERDA (2017). "Sucrose modulation of radiofrequency-induced heating rates and cell death". *Convergent Science Physical Oncology*. 3 (2017) 035001. DOI: 10.1088/2057-1739/aa757b.

John Paul Pineda, Charles Kim, Byong Kim, and Keibock Lee
Park Systems Inc., Santa Clara, CA USA

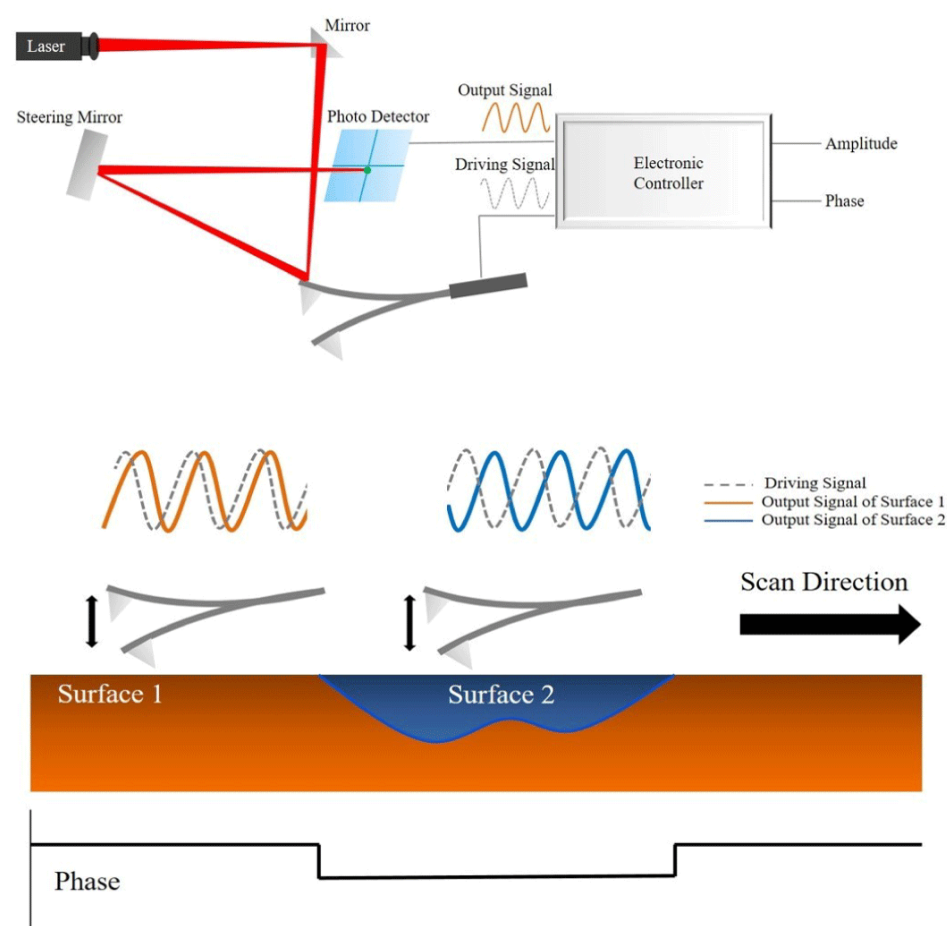


Figure 1. Schematic Illustration of Phase Imaging [6].

Introduction

Functional polymer thin films have numerous technological applications ranging from optoelectronics to sensors. Their tunable properties, flexibility, and low-cost preparation make them attractive to the industry. [1] The properties of polymer thin films are heavily affected by the distribution, shapes, and monomer composition of individual macromolecules. For this reason, designing polymer properties requires a characterization technique that can image material contrasts with high spatial resolutions to visualize the polymer morphology on the nanoscale and measure macromolecule sizes accurately. [2]

Scanning Electron Microscopy (SEM) and Energy-filtered transmission electron microscopy (EFTEM) are common methods to characterize polymer thin films. However, SEM has a low spatial resolution when imaging nanostructured organic samples containing light elements only, while EFTEM has high level of knock-on damage due to high accelerating voltages applied during operation. [3, 4] An effective tool to overcome these problems is Atomic Force Microscopy (AFM). AFM is a nondestructive technique that provides high-resolution images required for nanoscale characterization. Moreover, this tool can be operated in different measurement modes that image material

properties in addition to topological information. Among these, Phase Imaging is a powerful AFM mode used by scientists and engineers to study compositional heterogeneities in polymer materials. This mode provides complementary information to the topography image by revealing local variations of surface properties and compositions in the investigated materials.

In this study, a Park NX20 was used to characterize polymer thin films coated on Gold (Au) using Tapping Mode AFM. A high-resolution phase image acquired simultaneously with the topography image revealed that surface changes occurred after heating the sample and applying DC tip bias. The conformation and phase separation of the polymer domains were measured and evaluated.

Experimental

A polymer thin film coated on Au on a silicon wafer was heated up to 230 °C using a Park Systems temperature control stage. Additionally a 1 V DC voltage was applied between the AFM tip and the sample surface. With a Park NX20, both topography and phase image were obtained simultaneously by using Tapping Mode AFM under ambient conditions. Images were acquired before and after the sample had undergone the heating process and tip bias application. A conductive Mikromasch NSC36A Ti-Pt cantilever (nominal spring constant $k = 1$ N/m and resonant frequency $f = 90$ kHz) was used in the experiment.

Results and Discussion

In Tapping Mode, the tip oscillates near its resonance frequency, which allows the tip to periodically touch the sample surface at the lower turning point of the oscillation. Topography images are obtained by measuring the changes in the vibrational amplitude of the cantilever induced by the attractive Van-der-Waals force as the

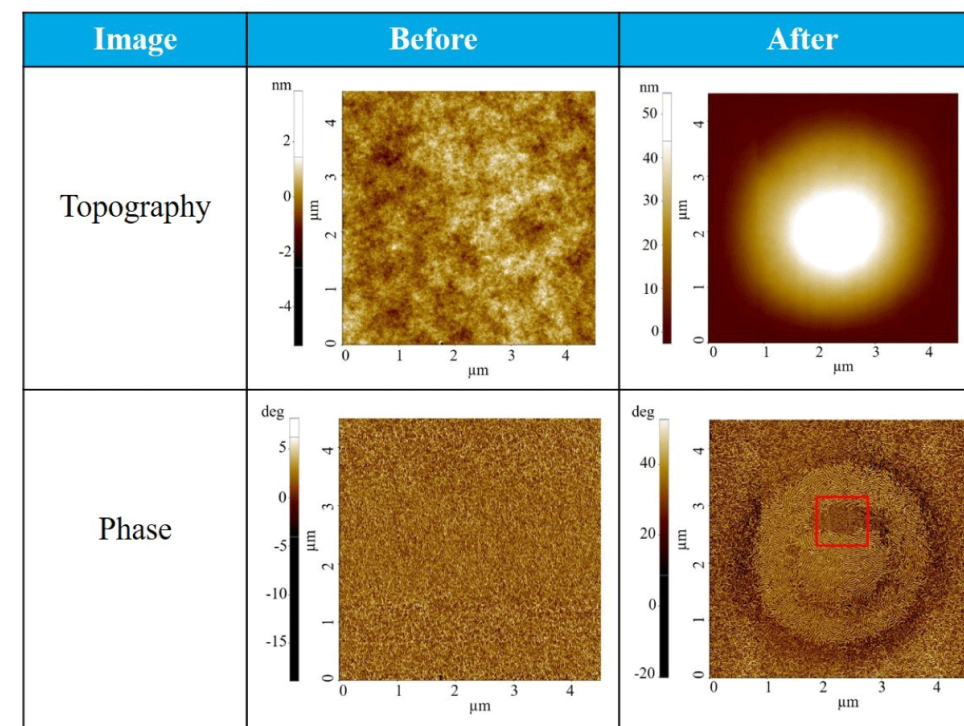


Table 1: Topography and Phase image before and after heating the sample at 230 °C and applying 1 V DC voltage between the sample and the tip.

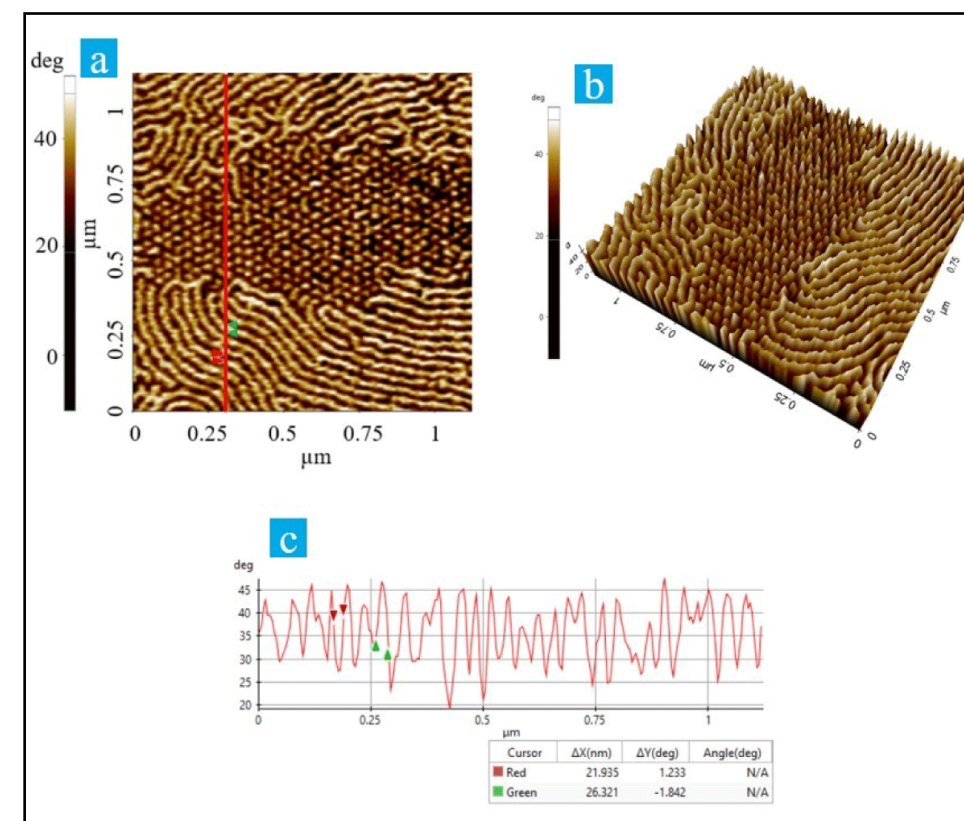


Figure 2. (a) Enlarged view of the phase image in table 1 (after heat and bias treatment), (b) 3D view of Figure 2a, (c) Corresponding line profile of Figure 2a.

cantilever is mechanically oscillated near its resonant frequency during the scan. The measured changes are compensated by the AFM's feedback loop, which

maintains the cantilever's constant amplitude and distance by controlling the Z scanner movement. [5] The phase image is acquired simultaneously by monitoring

the phase lag between the signal that drives the cantilever oscillation and its output signal, as shown in Figure 1.

Table 1 shows the topography and phase images of a polymer thin film before and after heating and bias application. The topography image acquired before the treatment reveals a smooth sample surface, while the phase image shows that the surface was composed of lamellar polymer fibrils distributed homogeneously over the surface. On the other hand, the topography acquired after the heat and bias treatment reveals that two circular protrusions (inner and outer protrusions) formed in the center of the scanned surface. The inner circular protrusion has a height of around 53 nm and a diameter ranging from 1.4 to 2.0 μm . The outside circular protrusion has a lower height of around 30 nm and a diameter ranging from 2.0 to 4.0 μm . The surrounding area is relatively flat with a mean square surface roughness of 0.8 nm. By comparing topography and phase image, it could be observed that the orientation of the lamellar fibrils in the inner and outer circular protrusions is re-arranged and the fibrils are aligned differently in both protrusions as well as the flat surface.

Figure 2a and 2b are the enlarged view and corresponding 3D representation of the area highlighted in red in the phase image of Table 1. Both images clearly show distinct differences in the fibril alignment. As such the upper and lower part of Figure 2a captured periodic fibrils align in-plane, while the dotted area in the center of the Figure corresponds to domains with fibrils that re-arranged in the vertical direction during the heat and bias treatment. Figure 2c is the corresponding line profile generated using Park XEI image analysis software to evaluate the sizes of the lamellar fibrils as well as phase separation. The measured width of the lamellar fibrils was approximately 26 nm, while separation between each fibrils was approximately 22 nm.

Summary

This study demonstrates the suitability of phase imaging for the characterization of polymer thin films. The high-resolution phase images obtained in the experiment reveals significant surface changes of the polymer thin films after they underwent

heating and bias application. It is observed that during the heat and bias application, some polymer fibrils re-aligned to a vertical orientation and others remained in-plane. Additionally, the in-plane fibrils formed domains of varying orientations. Thus, phase imaging can provide unique insights of how temperature and DC voltage affect the fibril arrangement and orientation of polymer thin films, as required to design customized properties. Since phase imaging operates in AFM tapping mode, this technique allows safe acquisition of high-resolution images without the continuous tip-sample contact. In sum, phase imaging is a promising tool in applications that require high-resolution imaging of material contrasts on the nanoscale.

References

1. S. Satish, et al., Preparation and characterization of nanoscale PMMA thin films Indian Journal of Pure & Applied Physics. Vol. 52, January 2014, pp. 64-67.
2. V. Korolkov, et al., Ultra-high resolution imaging of thin films and single strands of polythiophene using atomic force microscopy. Nature Communications volume 10, Article number: 1537 (2019)
3. J. Brostin, Compositional Imaging of Polymers Using a Field Emission Scanning Electron Microscope with a Microchannel Plate Backscattered Electron Detector. SCANNING Vol. 17, 327-329 (1995). Received March 13, 1995 and Accepted with revision May 22, 1995.
4. R. Masters, et al., Sub-nanometre resolution imaging of polymer-fullerene photovoltaic blends using energy-filtered scanning electron microscopy. Nature Communications volume 6, Article number: 6928 (2015)
5. [https://www.parksystems.com/images/spmmodes/standard/3_Phase-Imaging-and-Phase-Detection-Microscopy-\(PDM\).pdf](https://www.parksystems.com/images/spmmodes/standard/3_Phase-Imaging-and-Phase-Detection-Microscopy-(PDM).pdf)
6. J. Gunther, Introduction to Atomic Force Microscopy, March 10, 1998, ACS Group and MENS, Beckman Institute. <https://www.slideshare.net/joserabelo/atomic-force-microscopy-37962055>



Park Systems Announces \$1 Million Dollar Nano Research Grant Fund

If you are a researcher at a university or government startup lab you may be eligible for a Park Nano Grant. We started the Park Nano Grant program to support researchers that require atomic force microscopy equipment for their up and coming research.

Visit www.parksystems.com/grant to apply and learn more.



NanoScientific Symposium on Nano Applications for a Changing World

Covers applications in electrochemistry for clean energy, biotechnology for virus and cancer research for saving lives, and other nanomaterial studies for supporting better life.

"The science of today is the technology of tomorrow."
— Edward Teller

September 8, 2020

<https://parksystems.com/electrifiedbyAFM>

Join us for an Inspiring Symposium that Highlights Nano Applications & Research Leading Towards a Better Future

An Online virtual and interactive symposium on how NanoTechnology is Leading us Into a Better World.

Sponsored by Park Systems and NanoTechnology World Association and NanoScientific



NANOscientific

If you would like to present, submit your abstract to debbiewest@nanoscientific.org



MATERIALS MATTER

Column Highlighting Topics Presented in Dr. Advincula's Monthly Webinars on Advancements in Material Science



Dr. Rigoberto Advincula, Professor, Macromolecular Science & Engineering, Case Western Reserve University

The printed flexible electronics market is projected to reach \$330 billion by 2027 including different substrates from PET to polyamide to other flexible electronics, RFID tags, electronic paper, flexible solar cell, wearable electronics, sensors and different types of dynamic solid state and display devices, representation in logic, memory circuits, organic light emitting diode displays, and many others. The convergence of function and the ability to fabricate them in a high throughput manner is just going to grow and there's a lot of interest on wearable electronics.

What are flexible electronics? Wearable electronics represent different types of sensors that go directly onto your skin or implanted, such as sensing mechanism or textile and printed electronics on sportswear or gadgets that can be attached to what you wear every day.

What are the different types of flexible circuit structures? Flexible circuit structures can be divided into ratio geometries from single sided flex circuits, and then you build on top of this dielectric film features that can represent your circuit, your solid state display, your LCD, and an LED film or LED glass, would be a representation or several flexible automotive lighting composites that would typically be in a fabricator concept device. A double access flex circuit means there's a pattern on both sides of the substrate, with various methods to produce a finish, multi-material system with multi-layers circuits. A double sided flex circuit can represent flex circuits having two conductor layers, with or without plated two holes, depending on the design requirements, this will then

have a fabricated pattern and then a last deposited protective cover layer. The flexible circuits can be stacked to form multilayer flex circuits, building geometry and function in three dimensions. Rigid flex circuits are combinations or hybrid construction of this substrate, as well as metal layer construction on one side or both sides. And perhaps of higher interests in terms of bringing more polymer content into a flex circuit is the use of a polymer thick film as a substrate, a PTF. It simply means you can use polyethylene terephthalate, polyamides, polycarbonates and different types of roll throw plastic substrates that can produce high throughput fabrication methods.

What materials are used in flexible circuits? Flexible circuit materials are the base material for instance, a polymer film, would be called a laminate that can have a thickness anywhere from a 12 to 125 microns or five mils. This thin film can either be made of PET, polyamide, PEI, polyethyleneimine, or various types of polymers or even silicone polymers to control the chemical resistance and weapon behavior. Another material could be the deposition of a metal. A typical metal foil can be deposited either by printing or by electrolysis deposition methods. This means that you are able to create a pattern based on transfer of the metal material or a reduction of the metal on the surface.

What is the most manufactured device configuration? PCB is the most manufactured device configuration to integrate capacitors, resistors, and come up with a board that can be used for an instrument or automotive application.

There are several hierarchies in this type of manufacturing, which of course can be reduced into a printed or flexible electronics, if carefully designed, so in this level you will be looking at chips, chipsets interconnect scales.

How does nanostructuring and nanomaterials interface with flexible electronics? Nanostructuring simply means the ability to pick and place design and structure enables self-assembly of these nanomaterials, nanoparticles into a device that can be used either for optimizing an OLED or a sensor device. This can involve integrating an organic polymer material, whether it be the passive or the active component, or an inorganic material, including metal alloys and different types of high conducting materials, this becomes a hybrid system and not a composite. But putting this or integrating these all together requires an ability to synthesize, design and engineer this then on a nanoscale, positioning the patterning using a high vacuum environments ability to nucleate formation of these metals in a block copolymer composition or ability to control their self-assembly. Organic polymer materials give you a different hierarchy of ordering or supra molecular assembly. The orientation or even liquid crystal in behavior of different organic materials can be controlled.

This column is an excerpt from a webinar led by Dr. Advincula. The webinar also describes in depth research being done in Dr. Advincula's lab on future flexible electronics. To listen to the entire webinar, go to: <https://youtu.be/978mqMWZ47Y>

PARK SYSTEMS Announces \$1 Million Dollar

Nano Research Grant Fund for Researchers Setting up Nanoscience Labs in North America

(March 1, 2020) Park Systems, world-leading manufacturer of Atomic Force Microscopes announces a \$1 Million Dollar Nano Research Grant Fund to support researchers who are starting new nanoscience labs in North America. The Park Systems Nano Research Grant Fund provides up to twenty grants of \$50,000 towards the purchase of any AFM system and accessories manufactured by Park Systems.

“Park 50K Nano Research Grants align with our mission, “to enable nanoscale advances,” comments Keibock Lee, President of Park Systems. “We recognize that professors and scientists setting up their labs require the best scientific instruments, as they pursue new technology to improve our world. This is our way to help them achieve that goal.”

Park Systems started the Park 50K Nano Research Grant program to support researchers pushing the envelopes of nanoscale research and engineering with AFM equipment for their up and coming research as they pursue impactful science for the betterment of society.

“In every field - materials science, electronics, life science and nanotechnology, we keep up with the exhilarating pace of nanoscale microscopy and metrology innovations so scientists and engineers can focus on getting results,” adds Lee.

Park Systems \$1 Million Dollar Grant Fund offers new researchers setting up their labs easier access to the most advanced nanoscale technologies including atomic force microscopy, scanning ion conductance microscopy, and scanning electro-chemical microscopy tools, for applications ranging from materials science to in-vivo life science, electrical and electro-chemical research.



To complement its AFM equipment, Park Systems has a full line of options including acoustic enclosures, temperature control & environmental control, liquid cells, probe hands and other accessories such as a signal access module, electrical modules, external high voltage kits and magnetic field generators.

To qualify for a Park 50K

Nano Research Grant, you must be a university researcher or a professor of a national research university or a researcher at a national laboratory in North America starting a new nanoscience lab.

Please visit <http://www.parksystems.com/grant> to apply or to learn more. There are a limited number of grants, so apply early to ensure your opportunity to receive this assistance.

Park
SYSTEMS

Park Systems is a world-leading manufacturer of atomic force microscopy (AFM) systems with a complete range of products for researchers and industry engineers in the chemistry, materials, physics, life sciences, and semiconductor and data storage industries. Park's AFM provides the highest data accuracy at nanoscale resolution, superior productivity, and the lowest operating cost, thanks to its unique technology and innovative engineering. Cutting-edge AFM automation and nanometrology solutions provided by Park's team of 100% committed professionals improves workplace productivity. Park System Inc., headquartered in Santa Clara, CA has global manufacturing and R&D headquarters in Korea and is supported worldwide with regional headquarters in the US, Korea, Japan, Singapore, Germany, China and Mexico. Park Systems high-performance scientific instruments explore new scientific phenomena that enable scientists around the globe to contribute to impactful science that helps humanity grow and improve life standards.

Please visit www.parksystems.com/grant to apply and learn more.